8-2008

Experimental Studies of Electron Transfer between Wild Type and Mutagenic Cyanobacterial Cytochrome c_{553} and Photosystem I

Mehrsa Raeiszadeh
University of Tennessee, Knoxville

To the Graduate Council:

I am submitting herewith a thesis written by Mehrsa Raeiszadeh entitled "Experimental Studies of Electron Transfer between Wild Type and Mutagenic Cyanobacterial Cytochrome c_{553} and Photosystem I." I have examined the final electronic copy of this thesis for form and content and recommend that it be accepted in partial fulfillment of the requirements for the degree of Master of Science, with a major in Chemical Engineering.

Paul D. Frymier, Major Professor

We have read this thesis and recommend its acceptance:

Barry Bruce, Eric Boder

Accepted for the Council:
Carolyn R. Hodges

Vice Provost and Dean of the Graduate School

(Original signatures are on file with official student records.)

To the Graduate Council:

I am submitting herewith a thesis written by Mehrsa Raeiszadeh entitled "Experimental Studies of Electron Transfer between Wild Type and Mutagenic Cyanobacterial Cytochrome c_{553} and Photosystem I." I have examined the final electronic copy of this thesis for form and content and recommend that it be accepted in partial fulfillment of the requirements for the degree of Master of Science, with a major in Chemical Engineering.

Paul D. Frymier, Major Professor

We have read this thesis
and recommend its acceptance:

Paul D. Frymier

Dr. Barry Bruce

Dr. Eric Boder

Accepted for the Council:

Carolyn R. Hodges,

Vice Provost and Dean of the Graduate School

Experimental Studies of Electron Transfer between Wild Type and Mutagenic Cyanobacterial Cytochrome c_{553} and Photosystem I

A Thesis

Presented for the

Master of Science

Degree

The University of Tennessee, Knoxville

Mehrsa Raeiszadeh

August 2008

DEDICATION

This thesis is dedicated to my parents and sisters, who have encouraged me and showed me endless love. Without their support and patience, I would not have arrived here today.

ACKNOWLEDGEMENTS

I would like to express my deepest gratitude to my advisor, Dr. Paul Frymier, for his overwhelming guidance, patience, and the endless hours spent editing this draft. I feel very fortunate to have had him as my advisor, to have had the opportunity to work with him, and to have had his helpful advice for the past two years. He has been always available and willing to have a discussion with me, even on his busiest days. From the young graduate student, he led me though many challenges and transformed me. Working with him has made this journey very pleasant, and for that, I am deeply grateful.

An overwhelming thank you goes to my other research advisor, Dr. Barry Bruce. His experience, support, and encouragement have truly made a difference on my journey. Through all the meetings I had with him, I have always left his office happier, more encouraged and motivated and I am very thankful for that. I would also like to thank Dr. Eric Boder for agreeing to be on my committee. I would like to extend my gratitude to Dr. Bamin Khomami for providing me the opportunity to enter into Chemical Engineering Department and his caring attitude. An enormous debt of gratitude goes to Dr. Adam Taylor for his help and trust.

Certainly, this journey was not made alone. Through my struggles and successes my fellow group members shared my disappointments and joy. Here, I would like to extend my gratitude to Michael Vaughn, Natalie Myres, Ifeyinwa Iwuchukwu, Hillary Holback, Pinky Mahbubani, and Paul Willard. Extra special thanks must be given to Michael, Ify and Natalie, whose endless guidance and assistance were always there for me.

Friends have always been important to me. During my journey there was no shortage of great friendships. I would like to thank my friends; Cedric Tillman, Rachel Perkins, David Chang, Nick Casamatta, Katie Lamb and Minhea Kim. They have added laughter, happiness, and comfort to my journey. On this journey, it was difficult to be away from home. Although, I was away from my family, there was no shortage of love and support close to me. Here, I would like to express my thanks to Babak Zafari who helped and supported me like his sister. I would like to give special thanks to my best and special friend Sepideh Motamed. In the last two year of my life, the most difficult years, Sepideh was always there to encourage me, push me, and support me. Sepideh, thank you.

Last but not least, my love and gratitude go to my parents, Sima and Asad, for raising me with their ideal of always striving for excellence, for valuing my education and for putting my success and happiness the first priority in their lives. I am also grateful for their unconditional love and support at a great distance. I am thankful to my sisters, Saba and Mina, for advising me and showing me the path to success, and for their patience with their younger sister. Their love and encouragement has always been a constant source of comfort. I would also like to thank my cousin, Dr. Shokoofeh Moosavi, whose help and guidance were always there for me at the hardest time of my life.

ABSTRACT

A mutant form of the protein complex cytochrome c_{553} (cyt c_{553}) has been constructed by site-directed mutagenesis in *Thermosynechococcus elongatus* (*T. elongates*) to elucidate the binding and electron transfer properties between cyt c_{553} and photosystem I (PSI). The electron-transfer between wild type *T. elongatus* cyt c_{553} and a mutant form of cyt c_{553} and *T. elongatus* and *Chlamydomonas reinhardtii* (*C. reinhardtii*) PSI, has been studied as a function of cyt c_{553} concentration, ionic strength, pH and the detergents used to stabilize the protein. The effects of each of these variables were measured by an oxygen uptake assay. The mutated *T. elongatus* cyt c_{553} shows a higher electron transfer rate to *C. reinhardtii* PSI indicating that the insertion of acidic residues to the protein has facilitated the electrostatic interactions between cyt c_{553} and PSI. The effects of ionic strength and pH on the reaction indicate a strong influence of complementary charges on complex formation and stabilization.

TABLE OF CONTENTS

LIST OF TABLES

LIST OF FIGURES

CHAPTER 1

INTRODUCTION

1.1 Photosynthesis: Source of Sustainable Energy

Total annual global energy consumption is predicted to increase by 57% from 2004 to 2030 [1]. To date, nearly all domestic energy consumption has been provided by fossil fuels. Increased use of fossil fuels produces unacceptable levels of carbon dioxide, potentially bringing global warming, pollution, global energy inequity, and other issues. Atmospheric CO_2 levels, which were stable between 200 and 280 ppm for the previous 400,000 years, have risen sharply to 370 ppm since 1850 [2].

The potential for global warming makes it prudent that the development of zero-CO_2 emission fuels should be accelerated above the current development levels [2]. In addition, the rapid depletion of oil reserves will require the development of replacement fuels and infrastructure on the decades time horizon. Future fuels should not increase the amount of atmospheric CO_2, as fossil fuel combustion causes anthropogenic CO_2 emissions that may cause or increase global warming.

The capture and conversion of solar energy, the most abundant (178,000 TW $year^{-1}$) [2] and accessible renewable energy source, into chemical energy and biopolymers by photoautotrophic organisms is the basis for almost all life on Earth. Photosynthesis, the process by which plants harness the energy of the sun and convert it to chemical energy has provided virtually all of the world's chemical energy for more than three billion years, which to the present day has not been matched by any man-made technologies [2, 3].

Photosynthesis, the source of carbon that we burn in fossil fuels like gas and oil and of the carbohydrates in our food, can provide a new sustainable alternative energy source to fossil fuels by eliminating all of the very slow and inefficient processes between carbon fixation and the conversion of biomass into fossil fuel.

Artificial applied photosynthesis could offer a way to produce an efficient and sustainable energy source from solar power since sunlight is free, clean and very abundant. Photobiological hydrogen production could be an acceptable fuel production method if the cost were low enough because hydrogen can be produced renewably, is an efficient means of conversion sunlight energy to a fuel, and produces no green houses gases during its production or use in a fuel cell [4, 5]. Thus, using H_2 as a clean energy source seems to be promising [6-9].

1.2 Photobiological Hydrogen Production

Photobiological hydrogen can be produced by phototrophic organisms such as cyanobacteria and green algae from plentiful resources in nature such as sunlight and water [10-12]. This basic phenomenon has been known for 60 years [13, 14]. The cyanobacteria are prokaryotes that are capable of oxygenic photosynthesis; as bacteria, they are amenable to variety of genetic and molecular biological manipulations [15, 16]. These photosynthetic plants and bacteria contain various types of pigments, such as chlorophylls, bound to protein molecules that hold them in place. These pigments absorb and concentrate light energy but do not convert it to chemical energy right away. First, the light energy is used to transfer electrons to neighboring pigments; this sets in motion a series of other reactions.

The pigments and structures involved in photosynthesis are called reaction centers. In green algae and cyanobacteria, the conversion of light energy to chemical energy is driven by the cooperation of two light driven oxidoreductase reaction centers [17, 18]: the photosystem II (PSII) reaction center captures sunlight and splits water into molecular oxygen and hydrogen ions concomitantly providing mobilized electrons for the electron transport chain of oxygenic photosynthesis [3, 10, 19]; the photosystem I (PSI) reaction center is a large transmembrane multisubunit protein-chlorophyll complex that catalyzes the oxidation of reduced plastocyanin or cytochrome c_{553} which are located at the luminal side of the membrane [20-22]. After reduction of ferredoxin by PSI at the stromal side, the electron is transferred to ferredoxin-$NADP^+$ oxidoreductase, which reduces $NADP^+$ to NADPH that is then used for the fixation of carbon atoms in high energy bonds [12]. The electron transfer processes induce formation of a proton gradient across the membrane [19]. To accomplish this task, PSI uses light energy to generate a powerful reductant, $P700^{ox}$ (oxidized P700), that can transfer an electron to the primary electron acceptor, thus initiating electron transfer to $NADP^+$. P700, the primary electron donor of PSI localized near the lumenal surface of the thylakoid membrane is a chlorophyll species that in its excited state has a potential of approximately -1.2 V vs. SHE (standard hydrogen electrode) [23, 24]. Thus, $P700^{ox}$ is probably the most reducing compound found in natural systems [25]. Figure 1 summarizes the energetics and kinetics of the electron transfer processes in reaction centers of plants and different bacteria indicating that excited P700 is the most reducing compound in iron-sulfur and pheophytin-quinone type reaction centers [26]. P700 is the site of the light-induced charge separation of the photosystem in both cyanobacteria and higher plants [15].

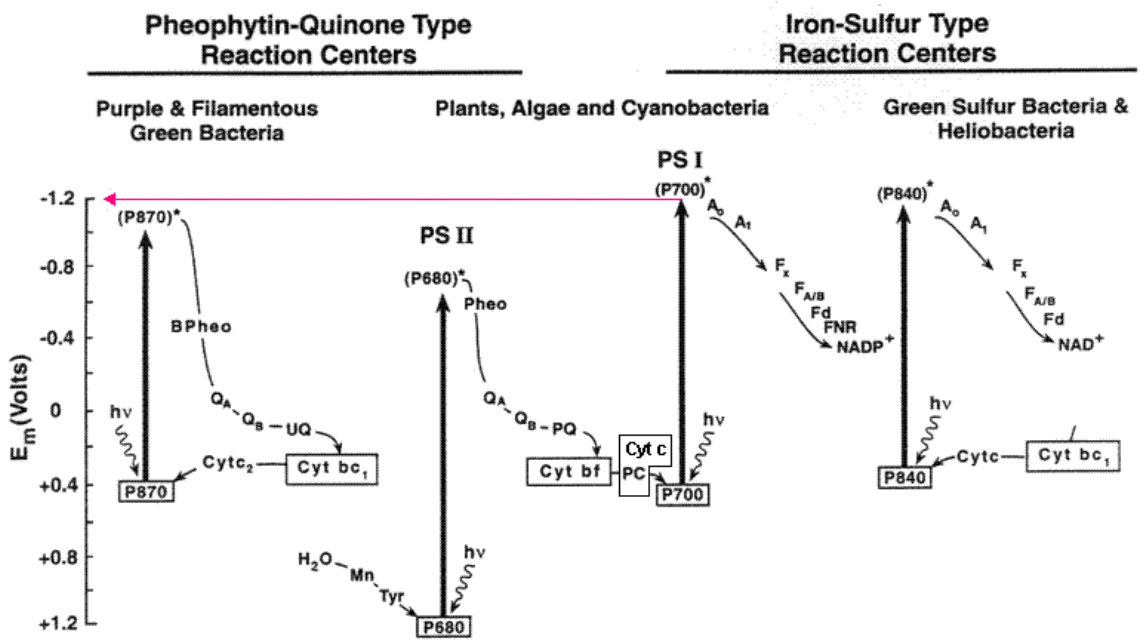

Figure 1: The Z scheme for electron transfer in oxygenic photosynthesis [26].

The electron generated by water-splitting is transferred from PSII to P700 via a pool of plastoquinones, the cytochrome (cyt) b_6f complex and a soluble electron carrier such as plastocyanin (Pc), or cytochrome c_{553} (cyt c_{553}) (Figure 2) [19, 27-30]. The cyt b_6f complex is an electron transfer and proton-translocating enzyme in oxygenic photosynthesis. It mediates electron transfer between Photosystem II and Photosystem I coupled to proton translocation across the chloroplast membrane [31, 32]. Electron transfer from the cyt b_6f complex to P700 occurs via a soluble electron transfer protein, either cyt c_{553} or Pc. Higher plants use Pc for this reaction, whereas some algae use either Pc or cyt c_{553} [15, 33]. Many cyanobacteria use only cyt c_{553} such as *Thermosynechococcus elongatus* (*T. elongatus*), and some have the ability to produce Pc [29, 34].

Pc is a small, blue copper protein which acts as an electron carrier between the cyt b_6f and PSI complexes in the photosynthetic electron transfer (ET) chain. Pc is located in the thylakoid lumenal, where it is freely diffusible in the lumenal space [26]. The photo-oxidized reaction center chlorophyll P700 in PSI is reduced by Pc and the oxidized Pc is in turn reduced by cytochrome f [15, 35-37]. In order to carry out its function, Pc must bind to cyt f, receive an electron, dissociate, diffuse to PSI, dock to a specific reaction site, donate an electron, and then dissociate again [26].

Depending on the relative availability of copper and iron in the culture medium cyt c_{553} can act as an alternative electron donor to P700. In the absence of copper, Pc is functionally replaced by the heme-containing protein cyt c_{553} [27, 30, 38-41].

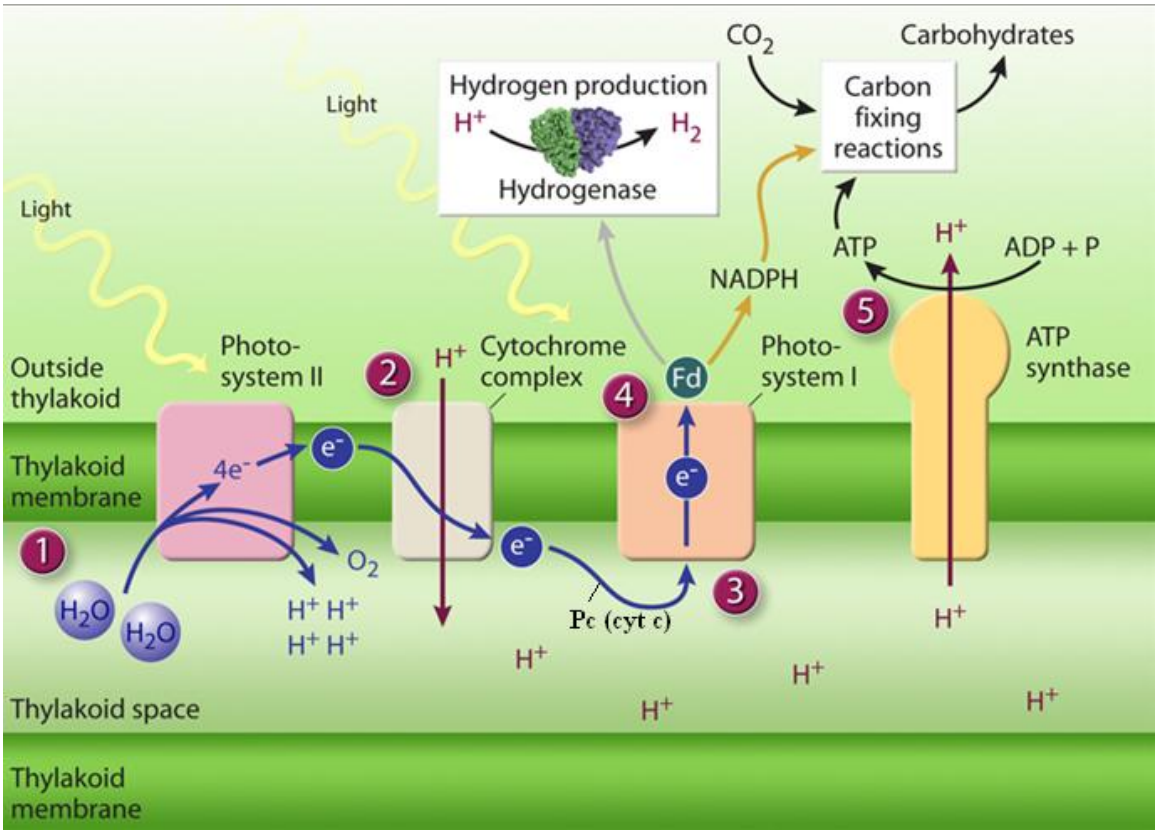

Figure 2: Genomics: GTL Roadmap, U.S. Department of Energy Office of Science, August 2005.

The cyanobacteria, which have the genetic ability to produce both Pc and cyt c_{553}, regulate the amounts of these two components based on the availability of copper and iron in the culture medium [15, 42].

1.3 Electron Transfer from Cytochrome c_{553} to Photosystem I

Electron transfer within and between cyt c_{553} and PSI is necessary for the function of photosynthesis. This electron transfer can be described by a multistep model of donor binding and oxidation and reduction reactions. Additional steps must be considered for interprotein reactions since these reactions are more complicated than the intraprotein electron transfer [43]. At least three distinct steps can be discerned for the electron transfer between Pc or cyt c_{553} and P700; formation of a transient complex between two redox partners, electron transfer within the complex, and the subsequent splitting of the product complex [41, 43]. However, the interpretation may be further complicated by the involvement of one or more conformational changes or rearrangements within the complex before electron transfer can take place. Accurately measuring the rate constants for each individual step is an important goal in this field [41, 43]. This thesis describes the electron transfer between cyt c_{553} and P700 of PSI and experimentally measures the effect of mutagenesis of *T. elongatus* cyt c_{553}, which has been modified in three specific residues located on the acidic part of cyt c_{553}, on this electron transfer. An appendix following the main text of the thesis describes an alternate methodology for measuring the rates of individual binding and intra- and interspecies electron transfer rates that is recommended for further studies of this system.

CHAPTER 2

BACKGROUND

Cyanobacterial PSI complexes interact very weakly and transiently with cyt c_{553} [30]; however they employ light harvesting complexes that are outside of the thylakoid membrane enabling the purification of PSI particles free from absorbing contaminants. Plants and algae have developed an additional cyt c_{553} binding site leading to faster electron transfer, but are very difficult to purify away from energetically uncoupled membrane-embedded light harvesting proteins. Therefore, it is desirable to introduce the cyt c_{553} binding site of higher plants into the thermophillic cyanobacterium *T. elongatus* in order to strengthen the interaction between the PSI complex and cyt c_{553}. The preference of *T. elongatus* is motivated by its temperature tolerance up to 95°C while the PSI complex *Chlamydomonas reinhardtii* (*C. reinhardtii*) will be denatured around 60°C [44]. It is anticipated that the thermophillic nature of *T. elongatus* reaction centers will offer greater stability of the hydrogen-evolving system over time, broaden the functional range of buffer conditions, and potentially result in increased hydrogen production rates when the temperature of the system is raised to the optimal growth temperature of the thermophile (approximately 55°C).

In *T. elongatus*, cyt c_{553} acidic patches are attracted to positive residues on PSI by long-range electrostatic forces to form an "electrostatic complex" which must undergo rearrangement before a suitable configuration exists for activation, leading to inter-protein electron transfer. Electron transfer from cyt c_{553} to excited P700 takes place in a complex between cyt c_{553} and PsaF subunit of PSI, after rearrangement from the initial

"electrostatic complex" to form additional, hydrophobic association of the northern area of cyt c_{553} with PsaA and PsaB of PSI [33].

The core of PSI is assembled from two partially homologous large protein subunits, PsaA and PsaB, containing the primary donor chlorophyll dimer, P700, the electron acceptors A_0 and A_1 as well as about 80 antenna chlorophyll molecules as are shown in Figure 3 [45, 46].

The terminal electron acceptors F_A and F_B are clusters of the stromal PsaC subunit. In addition to PsaC, the PsaD and PsaE subunits are shown to be located at the reducing side of PSI complex and to protrude into the stroma. PsaD is involved in the docking of ferredoxin to PSI. PsaE is important for efficient electron transfer to ferredoxin. On the oxidizing side of the PSI complex, the PsaF subunit is exposed to the lumen. It is involved in docking of cyt c_{553} or Pc reduced by cyt b_6f complex [45]. In eukaryotic organisms, binding of cyt c_{553} or Pc to PSI is mainly driven by two different forces, electrostatic attraction and hydrophobic contact. Long range electrostatic attractions between basic patches of PsaF and acidic regions of Pc or cyt c_{553} as well as the hydrophobic contact between the electron transfer site of the donors and PSI are required for stable electron transfer complex formation and efficient electron transfer [33, 35, 41]. The hydrophobic interaction site of the PSI core with the electron transfer donors is formed by PsaA and PsaB [19].

Previous studies indicate that the reaction mechanism of PSI reduction can be drastically modified by changing specific surface amino acids, mainly the acidic residues on the acidic part of the protein [38, 47].

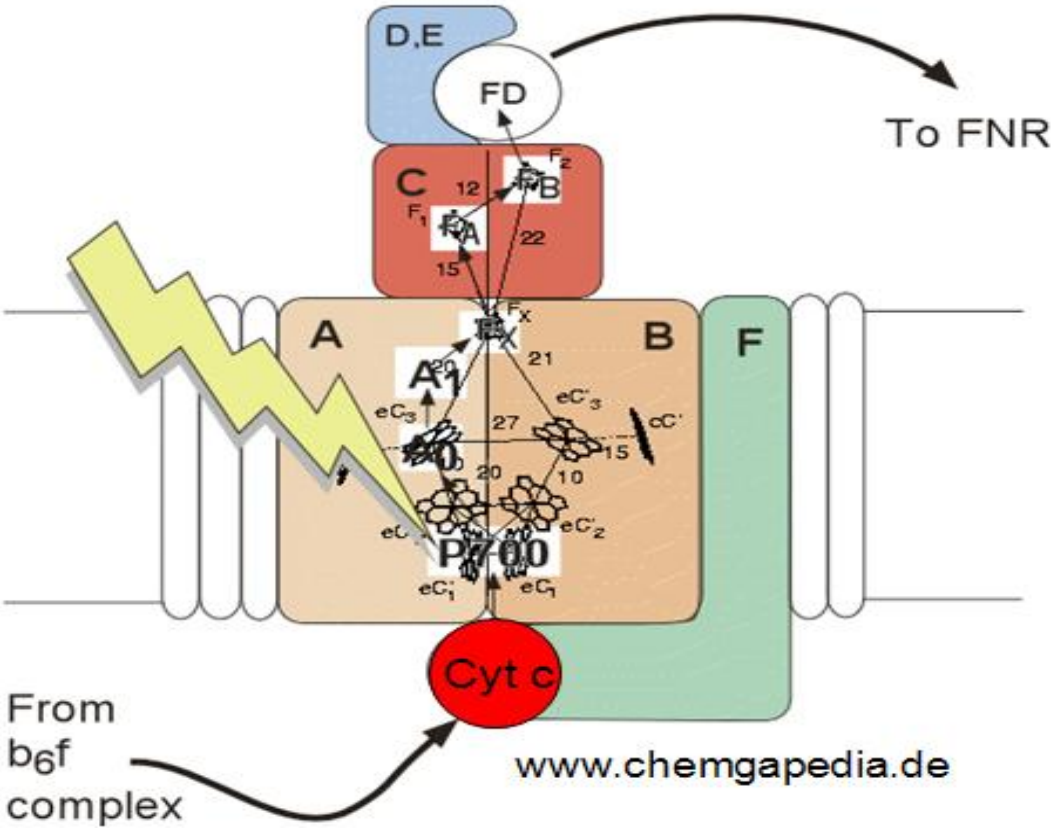

Figure 3: The reduced cyt c by the cyt b_6f complex docks with PSI for electron transfer to the $P700^{ox}$ special pair.

There are five important residues in *C. reinhardtii* cyt c for binding to P700 which are shown in Figure 4. E67, E68 and E69 are the key acidic residues for the interaction of cyt c_{553} with PsaF and D63 and R64 for the interaction with PsaB [41].The electrostatic interaction between the basic patches of PsaF and acid regions of cyt c_{553} as well as the hydrophobic contact between cyt c_{553} and PSI are crucial in effective electron transfer between cyt c_{553} and PSI [41]. E68 and R64, whose labels are shown in green in Figure 3, have been found to be analogous to those in cyanobacteria by structural superimposition. To investigate the importance of these residues, D63, E69 and E67 have recently been engineered into similar positions in cyanobacteria cyt c_{553} as in *C. reinhardtii* to increase the affinity of cyt c_{553} to interact with PSI. A cyt c_{553} site-directed mutant was modified by using standard molecular biology approaches; the details of these modifications will be discussed further in Chapter 3. The positions of these residues are listed in Table 1.

In Figure 4, panel A, *C. reinhardtii* PSI is shown in green (PDB ID: 1JB0), and the subunit PsaF in cyan with the proposed insertion in yellow. Blue are basic residues that recognize the acidic area on cyt c_{553} and form the interaction site for cyt c_{553} [38]. The electron transport chain is shown in orange, and the iron-sulfur cluster, where electrons end up before they leave PSI, is yellow-white. In panels B and C residues critical for cyt-PSI binding are displayed using space-filling models. The homolog of cyt c_{553} from *C. reinhardtii* is depicted in Figure 4 B showing acidic residues (E69, E70, and E71) and residues for interaction with PsaB (D65 and R66). In Figure 4 C analogous residues are identified for the acidic patch (D67, E68, and Q69) and the PsaB recognition element (G63 and R64).

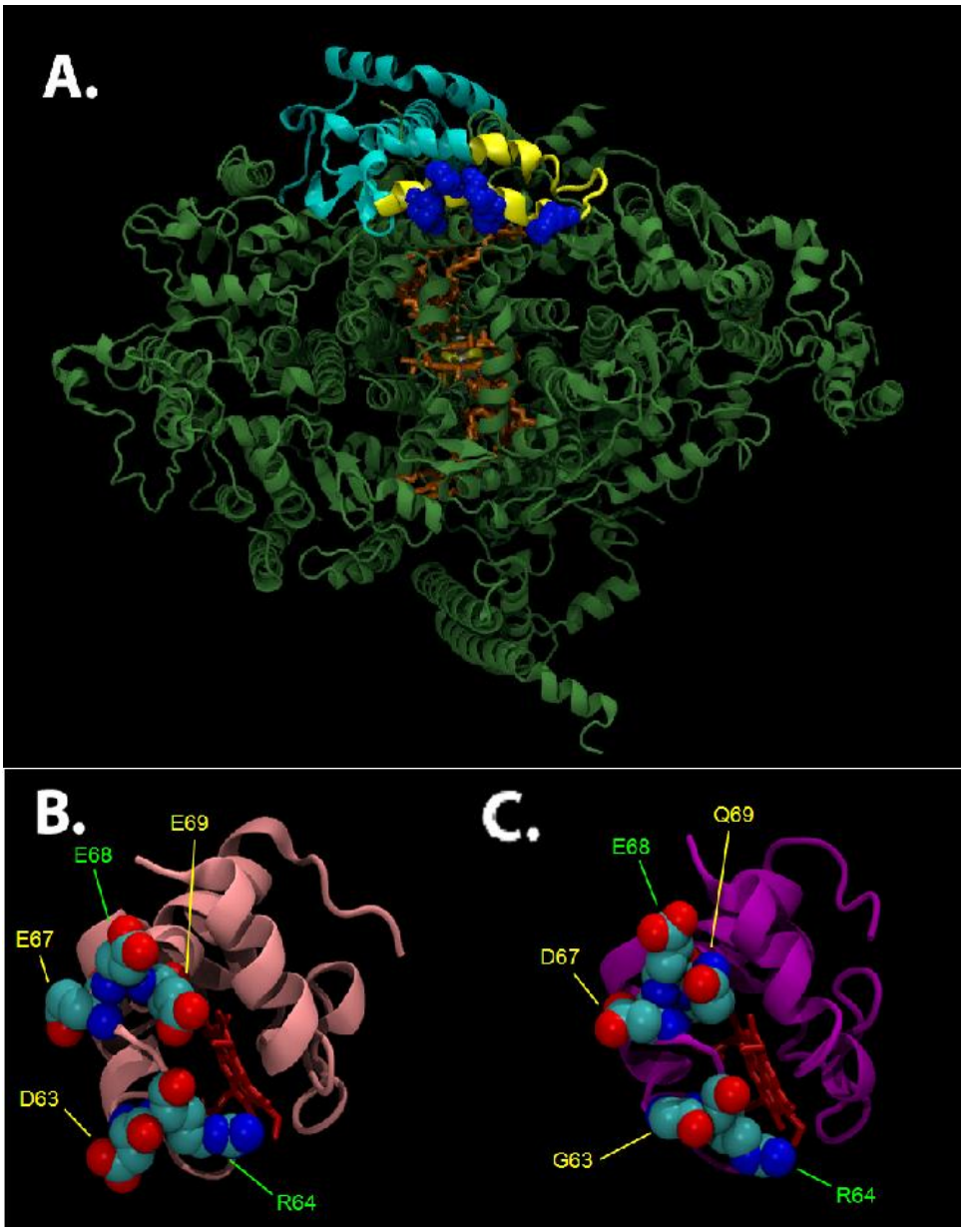

Figure 4: (A) *C. reinhardtii* PSI (B) *C. reinhardtii* cyt c_{553} (C) *T. elongates* cyt c_{553} (Picture prepared by M. Vaughn).

Table 1: Amino acid numbers of patches of *C. reinhardtii* and *T. elongates* cyt c_{553}.

Amino Acid Numbers	*C. reinhardtii* cyt c_{553}	*T. elongates* cyt c_{553}
63	Aspartic acid (D)	Glycine (G)
67	Glutamic acid (E)	Aspartic acid (D)
69	Glutamic acid (E)	Glutamine (Q)

CHAPTER 3

MATERIAL AND METHODS

In an *in vitro* system, PSI complexes can be reduced by wild-type or mutated cyanobacterial cyt c_{553}. The objective of this research is to compare and improve the kinetics of this electron transfer by homologous recombination. To evaluate the effect on overall electron transfer from cyt c_{553} to a terminal electron acceptor (methyl viologen dichloride hydrate (MV), in this case) through PSI, an assay in which oxygen uptake is measured has been done.

3.1 Respirometric Experiments

PSI particles from *T. elongatus* are supplemented with 2 mM Ascorbic acid Sodium salt (Asc) (Sigma-Aldrich) (to keep P700 reduced prior to illumination), 0.1 mM MV and 0.02% detergent (n-dodecyl-β-D-maltopyranoside (DM) (Sigma-Aldrich) and/or Triton) to prevent proteins precipitation. The presence of MV inhibits the recombination reaction between the electron acceptor side of the reaction center and $P700^{ox}$, as can be expected if MV is reduced by PSI [33, 48, 49]. Photo-oxidized P700 is then slowly reduced by Asc in a reaction which is greatly accelerated by adding increasing amounts of reduced cyt c_{553} or Pc. All experiments were done at 30°C. PSI reduces MV when supplied with Asc as an artificial electron donor to reduce PSI before the reaction starts [15].

$$
\begin{aligned}
&\text{Photo oxidation: } 2P_{700} \xrightarrow{h\upsilon} 2P_{700}{}^{+} + 2e^{-} \\
&\text{Donor side: } 2P_{700}{}^{+} + 2\text{cyt } c_{553} \rightarrow 2P_{700}{}^{r} \\
&\text{Acceptor side: } 2MV + 2e^{-} \rightarrow 2MV^{-} \\
&2MV^{-} + O_2 \rightarrow 2MV + O_2{}^{=} \\
&O_2{}^{=} + 2H^{+} \rightarrow H_2 0_2
\end{aligned}
\qquad (1)
$$

3.2 Respirometric Equipment and Instruments

Two biological oxygen monitors (YSI Incorporated, Model 5300) are used to measure oxygen uptake of the system, as shown in Figure 5. They offer recorder outputs for monitoring the results of each evolution of samples. These two channel instruments utilize Clark type polarographic oxygen probes. A thin membrane stretched over the end of the probe isolates the electrodes from the environment. The membrane is permeable to gases and allows them come in contact with the probe face. When a voltage is applied across the electrodes, oxygen will react at the cathode causing a current to flow. The probe actually measures the pressure of oxygen outside of the membrane since it is assumed that the oxygen pressure inside the membrane is zero due to the rapid oxygen consumption at the cathode. Thus, the force causing the oxygen to diffuse is proportional to the absolute pressure of oxygen outside of the membrane. These probes are immersed in magnetically stirred sample chambers. The bath provides relatively air-tight sample chambers which are temperature-controlled in by an external water bath. The four sample chambers are held in place with locking nylon hold down rings and sealed in the bath with two rubber o-rings [50]. All samples are prepared under safe lights (transmission maximum 520 nm) to avoid extraneous excitation of PSI. All the assays are carried out in 3.35 ml of reaction volume in glass cuvettes at 30°C. The volumes of cuvettes were determined by multiplying the measured weight of cuvettes containing water by the

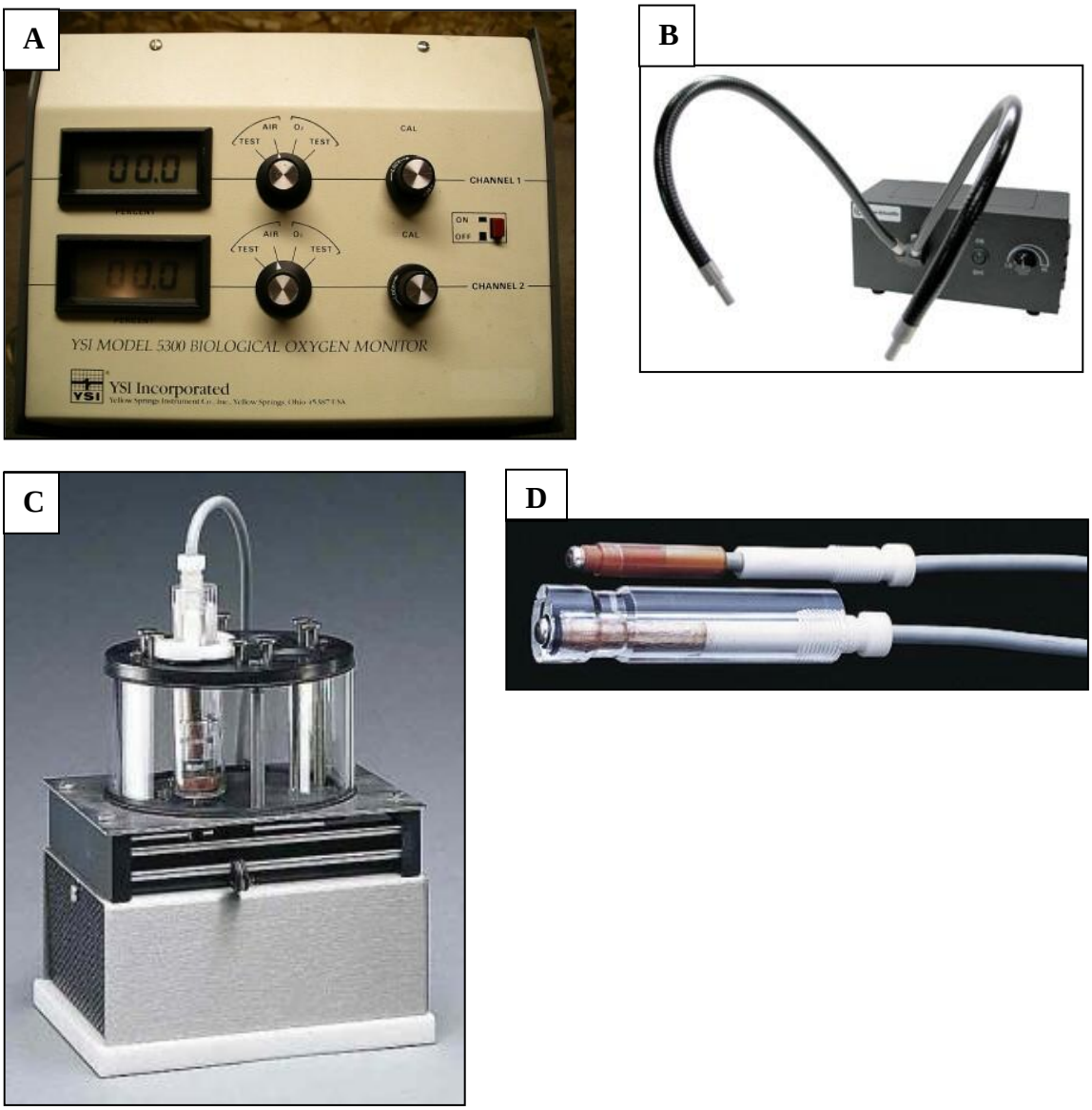

Figure 5: A. an YSI model 5300 biological oxygen monitor (Figure from labextreme website, June, 2008, http://www.labextreme.com) B. a light source with guides (Figure from Fishersci website, June, 2008, http://www.fishersci.com) C. YSI Chamber (Figure from Cole-Parmer website, June, 2008, http://www.coleparmer.com) D. YSI Clark electrodes (Figure from Cole-Parmer website, June, 2008, http://www.coleparmer.com)

Table 2: Volumes of YSI chamber cuvettes.

Cuvette Number	Volume (ml)					
	Test 1	Test 2	Test 3	Test 4	Test 5	Test 6
1	3.32	3.32	3.42	3.38	3.37	3.36
2	3.41	3.49	3.39	3.36	3.47	3.38
3	3.52	3.39	3.35	3.24	3.26	3.41
4	3.21	3.32	3.43	3.38	3.25	3.32
Average						3.35

molecular weight of water. 3.35 ml is the average of 6 measurements performed on each cuvette. The results are shown in Table 2.

All the electrodes are calibrated under aerobic conditions with constant stirring in the dark and the reading on the amplifier is set to 100.0% saturation by oxygen in air at these conditions. Samples are allowed five minutes of darkness and exposure to atmospheric oxygen (in ambient air), prior to their introduction to light, perpendicular to the sample tubes. Two halogen lighting units (21 volts, 150 watts, Model EJA, General Electric) with 2 light guides per lighting unit are used to illuminate the samples in the sample chambers. The light apparatus is lowered around the 4-sample tube water chamber, and fitted flush with the chamber (Figure 6). The apparatus is shown in Figure 6. In this configuration, a sample located at position 1 is always associated with the electrode labeled 1, and has an electrode output to one of the oxygen monitors, denoted device 1. These three elements form set 1. The remaining tube positions, electrodes and electrode outputs are connected in a similar manner, and form sets 2 through 4. Samples

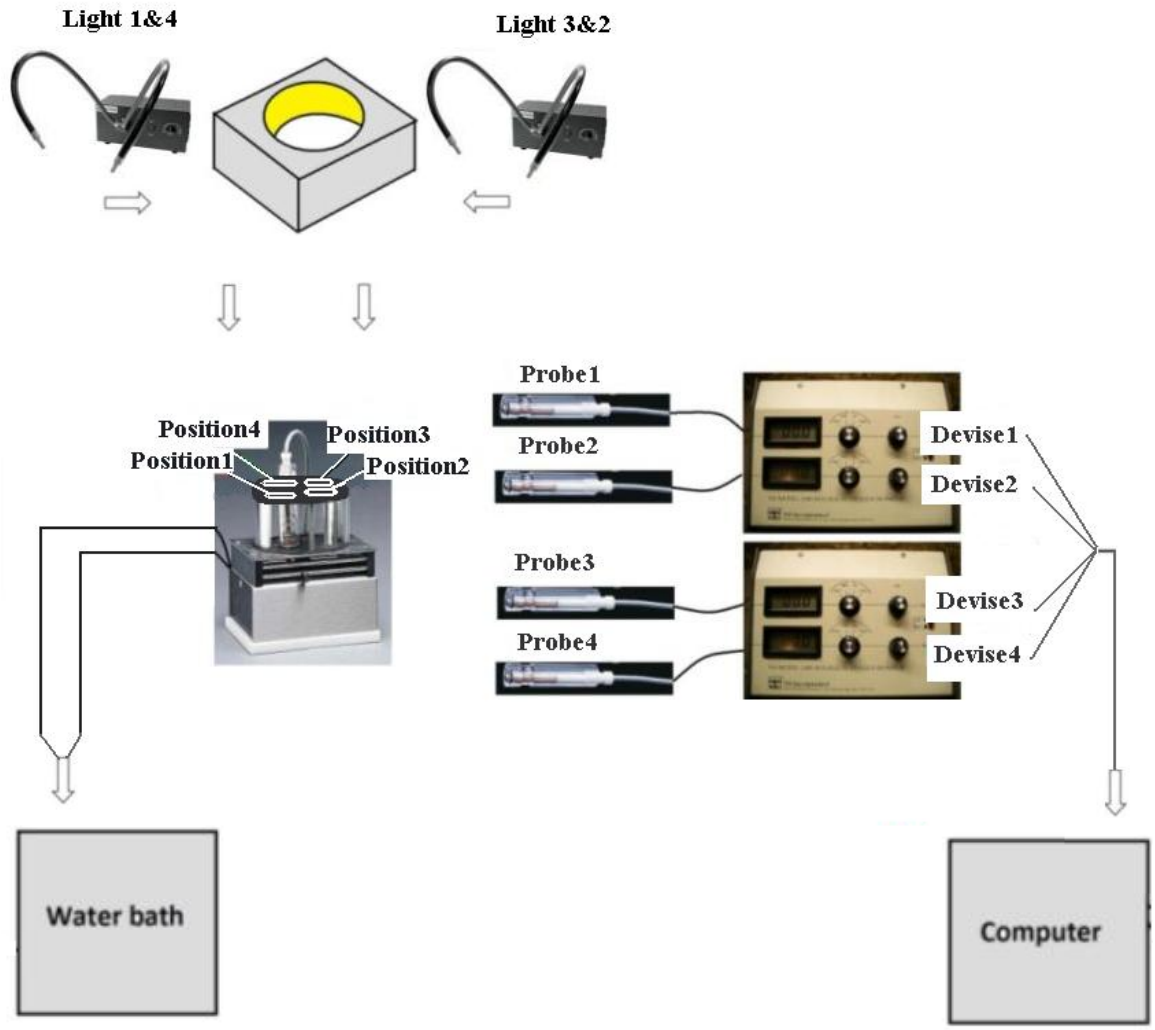

Figure 6: Schematic of respirometric apparatus configuration.

are continuously mixed during data collection. Oxygen uptake is directly obtained (as an electrical signal proportional to the percent oxygen remaining in solution) from the oxygen monitors. Data on the oxygen concentration (as a percentage of atmospheric oxygen saturation) for each PSI/cyt c_{553} sample are collected with an analog-to-digital signal converter (National Instruments, model USB-6211) and stored on a computer.

Upon the start of the reaction, the oxygen concentration is measured at 0.1-second intervals for 4 minutes, defining the oxygen uptake curve. The raw data is stored as percent oxygen saturation from air as a function of time. Oxygen uptake rates for each sample are determined from linear regressions of the oxygen concentration as a function of time. Regressions are determined over the portion of the curve where the slope deviates from the baseline (that is the oxygen concentration before the lights were turned on, which was essentially constant at 100% saturation). To determine the actual oxygen consumption rate, the percent oxygen saturation is converted to moles of oxygen in the following way. An air-saturated aqueous sample at 1 atmosphere and 30°C contains 5.46 μl O_2/ml (see Table 3) [50]. If the oxygen concentration changes from 100.0% to (100.0-X)% in t seconds, the air saturation is reduced by X%. A saturation change of X% in t seconds means X% × 5.46 × 3600/t μl O_2/hr/ml H_2O. The X value for each experiment is collected from 100.0% for the duration of either 50 seconds or 100 seconds depending on the concentrations of materials which effect on the rate of oxygen uptake. To obtain the rate of oxygen uptake in μ mol O_2 / (mg chlorophyll × hr) the following equation is used:

$$\frac{\mu\text{l O}_2}{\text{hr}\times\text{ml}}\times 1.2875\,\frac{\text{g O}_2}{\text{l O}_2}\times\frac{\text{mol O}_2}{32\text{ g O}_2}\times\frac{1}{\text{M PSI}}\times\frac{\mu\text{M PSI}}{96\mu\text{M chl}}\times \frac{\mu\text{mol chl}}{893\mu\text{g chl}}\times\frac{10^3\,\mu\text{g chl}}{\text{mg chl}} = \frac{\mu\text{mol O}_2}{\text{mg chl}\times\text{hr}}, \tag{2}$$

Table 3: Volume of oxygen dissolved in water microliters O_2/milliliters at 1 atm [50].

Temp. °C	Equilibrated with Air (21% O_2)
	H_2O
15	7.18
20	6.51
25	5.98
28	5.65
30	5.48
35	5.14
37	5.02
40	4.85

where 1.2874 g/l is the density of oxygen at 30°C is calculated using the ideal gas law and "M" is the mass of PSI in micromoles.

3.3 Cyt Subcloning and Mutagenesis

All the genetic transformations for this work were carried out by Natalie Myers, MS candidate in Microbiology at the University of Tennessee. The author of this thesis is grateful for this critical contribution to this work. The methods used by Ms. Myers are described in the following sections.

3.3.1 Introduction

The *T. elongatus* genome has 2.6 million base pairs; its cyt c_{553} gene (pet J) has 339 base pairs which code for 112 amino acids and one stop codon, as shown in Figure 7. The pet J cytochrome gene codes for an immature, 112 amino acid preprotein with a 25 amino acid signal peptide. After cleavage of the signal peptide the mature apoprotein cyt c_{553} has

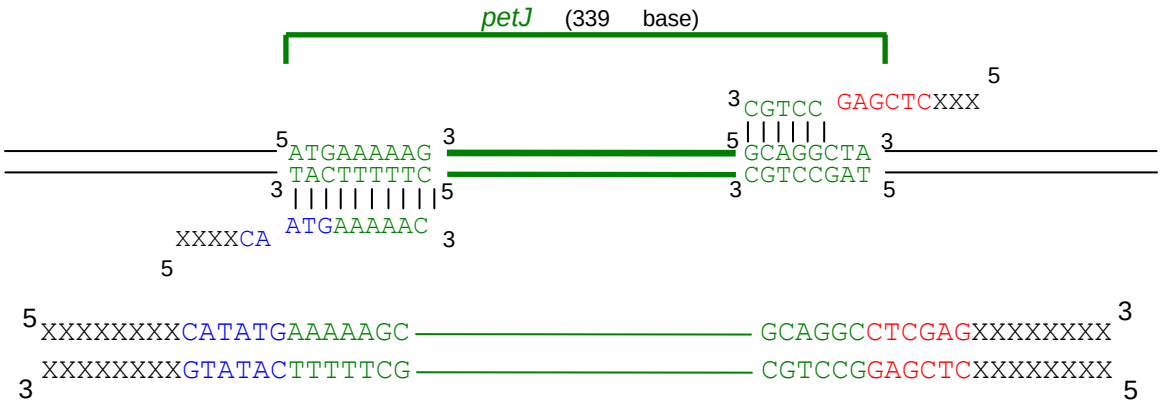

Figure 7: pet J gene from *T. elongatus.*

87 amino acids. The holoform of the protein is formed by the addition of a heme protein to the apoprotein. In order to isolate the genomic DNA of cyt c_{553} *T. elongatus* cultures are grown to log phase in NTA media and cell lysis and genomic DNA isolation is performed [51].

3.3.2 PCR (Polymerase Chain Reaction) Amplification

In order to make copies of the gene of the interest, pet J, two gene-specific primers with 25 base pairs are ordered to anneal to pet J gene. These primers go to the ending sites of the pet J gene that they have homology with and bind with them.

The DNA polymerase enzyme that are already added start synthesizing the primers towards each other and produces single strands of DNA. When these strands meet the end of the pet J gene, synthesis stops. The complementary strands then anneal together. After extension primers are separated from the genomic DNA and free to anneal to one another based on their complimentary ends and PCR fragment/product has been produced. After separation of PCR fragments from the genomic DNA, new primers can bind to the genomic DNA and make more PCR fragments.

After cloning the full-length sequence for the cyt c_{553}, restriction enzymes NdeI and AvaI can be used to digest the PCR product and make sticky ends. The same restriction enzymes are then used to digest the pET30b (the circular vector plasmid) and generate a linearized vector with complementary ends to the ends that has been formed in the PCR product, as shown in Figure 8. pET30b confers kanamycin resistance and includes a C-terminal 6x:His tag on the expressed protein which is used to facilitate purification of the protein by affinity chromotography. Standard subcloning techniques are used to ligate the insert DNA with the digested vector. By subcloning the PCR product into the pET30b vector, pET-TEC553 is obtained.

The product with sticky ends is ligated to the linearized vector plasmid to obtain the final plasmid. Circular plasmids developed as described above have the following advantageous properties:

1. The gene of interest is under inducible expression. IPTG for promoter translation is located inside *E. coli* which induces expression.
2. Having the gene in a circular plasmid is advantageous for manipulation:
    a. Grow a lot of the plasmid for lots of copies for later transformation
    b. It is advantageous for mutagenesis which will be discussed later
    c. Many cells with *E. coli* included will only take up circular DNA during transformation.
3. Introducing the antibiotic selection on the plasmid controls the ability to recover only the *E. coli* cells that have taken up the plasmid with pet J gene during the transformation.

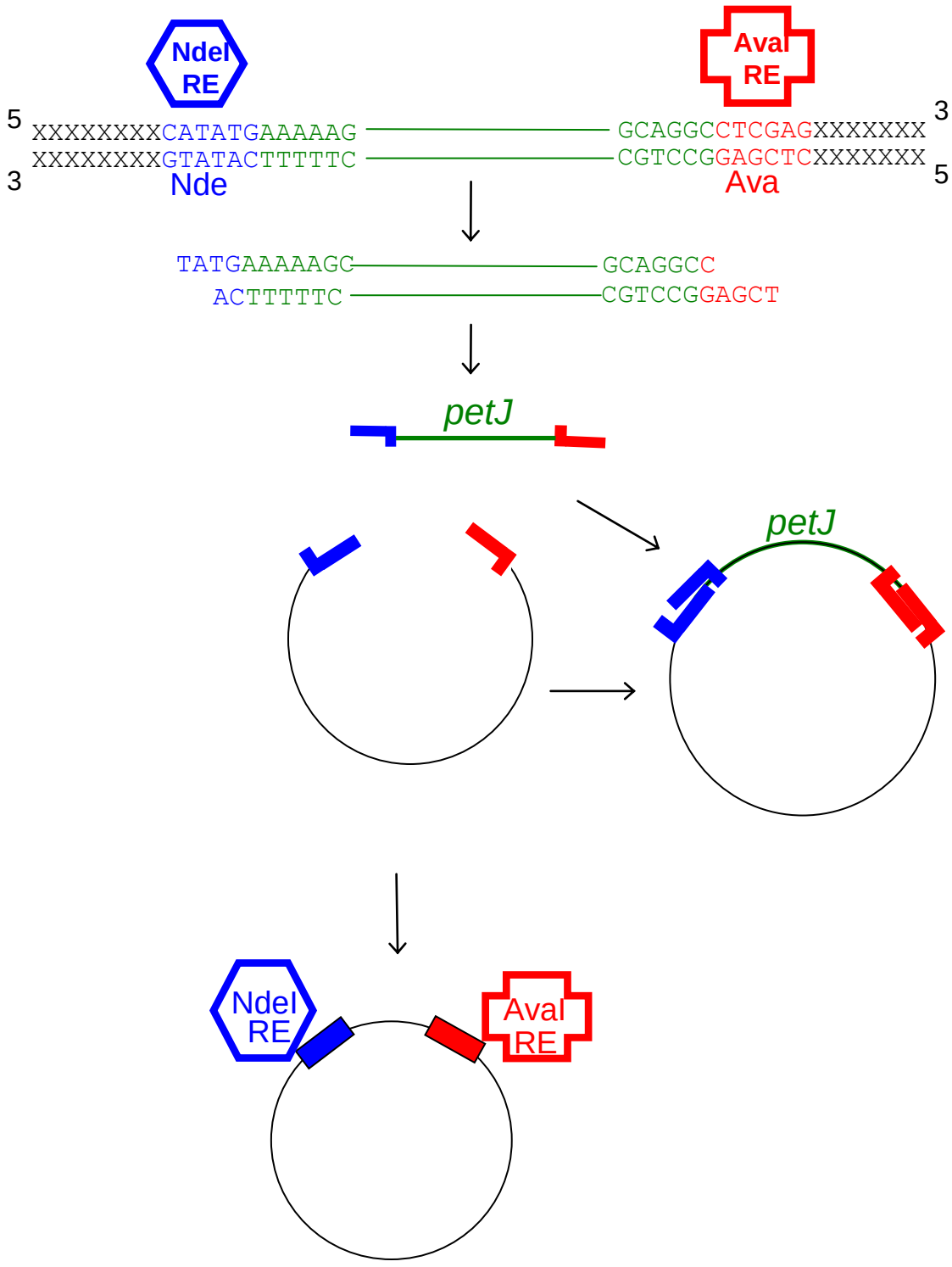

Figure 8: Digestion of the cloned cyt c_{553} sequence/pet J gene and pET21b vector by restriction enzyme and production of pET-TEC553.

3.3.3 Transformation

After the plasmid has been constructed, it is then transformed into a cloning strain; *E. coli* NB in this case. First, *E. coli* cells are incubated with high calcium concentration in the Nova Blue (NB) buffer which makes the membrane porous. Cloning strain NB is utilized to amplify the amount of created plasmid. Cells are kept on ice and the complete plasmid, pET-TEC553, is transformed into *E. coli* cell in the absence of antibiotic. After incubation for 30 minutes, cells are transferred into a water bath at 42°C to close the membrane pores. Then, *E. coli* cells with the vector plasmid including the antibiotic resistance genes; kanamycin and ampicillin are plated and grown in LB (Luria-Bertani) nutrient broth in the presence of antibiotics. Ampicillin is added for co-expression of cyt c_{553} maturation proteins which facilitate heme insertion. Therefore, only the *E. coli* cells that have taken up the plasmid with the pet J gene and antibiotic resistance genes survive. For cyt expression, the plasmid DNA is transformed into the expression strain *E. coli* PE3 (RIL). Cultures are grown in SV medium (limited nutrient medium, which enhances expression of cyt) in the presence of kanamycin and ampicillin. After a desirable concentration of cyt is reached, cultures are induced with IPTG and transcription of pet J gene starts. The 112 amino acid preproteins are expressed in the cytoplasm of the *E. coli* cells. The signal peptide targets the preprotein into the inner membrane of *E. coli* for secretion to the periplasm, the space between inner membrane and very outer most membrane, through the Sec apparatus because heme insertion proteins are located in periplasm. After the preprotein gets to the Sec system proteins on the inner membrane, its signal peptide cleaves off. Heme insertion occurs in the periplasm via heme insertion proteins and the mature holoprotein with 87 amino acids is

produced. Heme insertion proteins are responsible for the energy-independent ligation of heme into the cyt apoprotein.

After collecting the cells, the outer membrane is sheared away by two freeze/thaw cycles and formation of ice crystals to aid recovery of the protein from the periplasm. The final product after the freeze/thaw cycles is spheroplast, which contains the inner membrane and cytochrome-containing cytoplasm.

3.3.4 Purification

Immobilized Metal Ion Affinity Chromatography (IMAC) is used to purify cyt c from all *E. coli* proteins. The total periplasmic fraction is passed over the chromatography column with Ni charged sepharose beads. His tag residues attached to the end of the cyt c protein are taken advantage of for purifying cyt c from all *E. coli* proteins. Cyt c binds to the beads via the affinity of cyt c His tag for Ni and all other contaminating proteins flow past. Then imidazole is used to elute the purified/separated cyt c. Sodium dodecyl sulfate polyacrylamide gel electrophoresis (SDS/PAGE) is used to confirm the purity of cyt according to its electrophoretic mobility. After IMAC purification, the cyt c is subjected to Tris-Tricine-SDS as described by Schagger and Von Jagow [52]. To summarize, there are 5 steps taken for subcloning the cyt c_{533}:

$\xrightarrow{1}$ Prepare pET Vector (Digest with restriction enzyme) $\xrightarrow{2}$ Prepare Insert DNA (Restriction digest) $\xrightarrow{3}$ Clone Insert into pET Vector (Anneal insert with pET vector) $\xrightarrow{4}$ Transform into Expression Host $\xrightarrow{5}$ Induce and Optimize Expression of Target Protein $\xrightarrow{6}$ Scale-up, Purify Target Protein [53]

3.3.5 Site-directed Mutagenesis

In order to manipulate the plasmid DNA to code for desired amino acids the plasmid with target sites for mutation is denatured and anneal to the primers containing the desired mutation. As shown in Figure 9, primers are complimentary to the gene sequence on both sides of the mutation site but introduce different nucleic acids at the mutation sites, and amino acid substitutions are introduced based on the *C. reinhardtii* model. The DNA polymerase enzyme starts synthesizing and extends the mutagenic primers resulting in nicked circular strands. After the synthesis of the mutated DNA is completed, a restriction enzyme (Dpn I) is used to digest the nonmutated parental DNA template. Then, the circular nicked DNA is transformed into XL1-Blue supercompetant cells. After transformation the XL1-Blue supercompetant cells repair the nicks in the mutated plasmid [54].

3.4 PSI Isolation

3.4.1 C. reinhardtii PSI Isolation

The cells were washed in 50 mM HEPES, pH 7.2, 5 mM $MgCl_2$, 5 mM $CaCl_2$, 20% glycerol (v/v) to remove secreted proteins out of the cells and collected after 15 minutes centrifugation at 9000*g*. Cells were again washed in the same buffer containing 1 mM phenyl methyl sulfonyl fluoride (PMSF), 1 mM EDTA and 1 mM benzamidine to inhibit protease and centrifuged. The membranes were mechanically lysed in a chilled French press at 660 kg/cm^2 pressure. Unbroken cells and starch granules were removed from the membrane suspension and the cytosolic proteins and the contents of cytosol were collected by centrifugation at 2000*g* for 5 minutes.

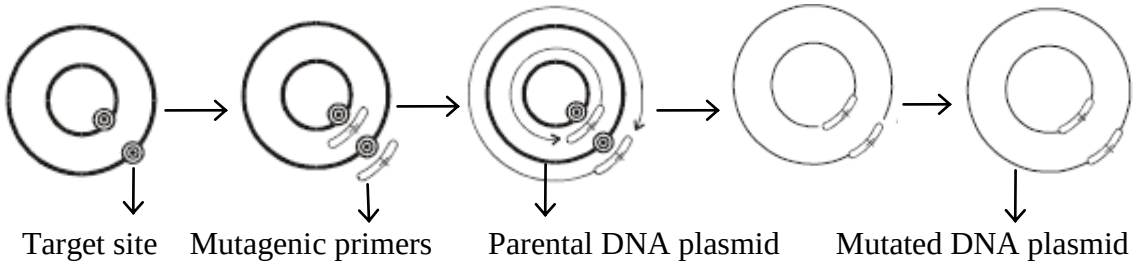

Figure 9: Site directed mutagenesis method [54].

The crude thylakoid membranes in the supernatant were pelleted by centrifugation at 100,000 *g* for 20 minutes and cytosolic proteins were removed. After washing the cells in the same buffer containing EDTA and benzamidine, the thylakoid membranes are solubilized with 0.6% solution of DM (Dodecyl Maltopyranoside) in the dark for 15-20 minutes on ice with gentle stirring. The suspension was then centrifuged at 125,000 *g* for 20 minutes and all the unsolubilized membrane materials in the pellet were removed. All the solubilized chlorophyll containing membrane proteins; PSI, PSII, LHC complexes, ATPase and cyt b_6f in the supernatant were collected. To separate PSI from all other proteins the supernatant was loaded onto a POROS HI column (150 mm $\times$ 4.6 mm, a weak anion exchanger). 1 ml fractions were collected using a fraction collector. The hlorophyll concentration in the supernatant was determined by measuring the absorption with a spectrophotometer at 645 and 663 nm using the following equation (31):

$$\text{Total Chlorophyll} = \text{Chl a} + \text{Chl b} = (20.2 \times A_{645}) + (8.02 \times A_{663}) \quad (3)$$

3.4.2 T. elangatus PSI Isolation

The frozen cells were resuspended in the wash buffer containing MES pH 6.5, 5 mM $CaCl_2$ and 5 mM $MgCl_2$ and centrifuged. The pellet was resuspended in lysis buffer

containing MES, $CaCl_2$, $MgCl_2$ and 500 mM sorbitol. The resuspended cells were adjusted to a chlorophyll content of 1 mg/ml [55] and homogenized using a Dounce homogenizer. For lysozyme treatment, solid lysozyme was added to the suspension to 0.2% (w/v) and the mixture was incubated in the dark at 42°C for two hours. The resulting mixture was centrifuged as before and the supernatant was discarded. The pellet was resuspended in the wash buffer. The volume was adjusted so that the chlorophyll concentration was 1 mg/ml. The cells were lysed by passing through a French press three times at 1758 kg/cm^2. To wash the membrane fragments, all of the lysate was collected and centrifuged at 20,000 rpm in a Sorvall centrifuge with a SS-34 rotor for 20 minutes. The supernatant was discarded and the pellet resuspended with wash buffer and centrifuged as previously described. The pellet was resuspended in wash buffer including 3 M NaBr and the supernatant was discarded. In order to solubilize the washed membrane fragments, the pellet was resuspended in DM and incubated at 20°C for 20 minutes with gentle stirring. Then, to collect insoluble material, sample was centrifuged in the SS-34 at high speed for 30 minutes [55]. The supernatant was separated from the pellet and then loaded onto 10-30% sucrose gradients with 60% cushion, all the gradient solutions also contained 20 mM MES and 0.03% DM. The sucrose density gradient centrifugation was done overnight 14-18 hours at 24,000 rpm in a SW-28 at 10°C to separate PSI from all other proteins. The lower green band was collected and pooled after centrifugation with a 4 inch, 14 gauge stainless steel needle. The HPLC was performed on the lower green band containing 20 mM MES pH 6.4, and 0.03% DM as described by Fromme and Witt [56].

To measure the chlorophyll content of the collected PSI, the absorbance of the sample was measured at 665 nm by spectrophotometer. The following equation relates the amount of chlorophyll a in the sample:

$$\mu\text{g Chl a / ml} = A_{665} \times 13.9 \quad (4)$$

3.5 Isolation of Genomic DNA from *T. elongatus*

T. elongatus liquid cultures were harvested to achieve a cell pellet after grown to log phase in NTA media. Cell lysis and DNA isolation were performed as previously described [51]. The pellet was incubated in 100 mM Tris and 10 mM EDTA (pH 8) with 25 mg/ml lysozyme at 37°C for 80 minutes. 10% SDS was added to the sample, after which it was vortexed and incubated at 25°C for 10 minutes. 20 mg/ml proteinase-K was added and incubated at 65°C for 60 minutes. Lysate was neutralized with 3M potassium acetate (pH 5.5) and incubated on ice for 4 minutes. Cell debris was pelleted at 10,000 *g* for 10 minutes at 25°C. The Lysate supernatant was transferred to a new microcentrifuge tube and saturated buffered phenol: chloroform: iso-amyl alcohol (24:24:1) was added and centrifuged at 14,000 *g* for 4 minutes. The clear aqueous solution and white middle layer was transferred to a new microcentrifuge tube and the purification was repeated once. Chloroform: iso-amyl alcohol (24:1) was added to the clear aqueous solution and centrifuged as above. The DNA contained in the aqueous portion was precipitated upon addition of chilled 100% EtOH, and incubation at -20°C for 60 minutes. Precipitated DNA was pelleted at 14,000 *g* for 15 minutes, after which EtOH was aspirated from the pellet. Pellets were left exposed to air for drying and then resuspended in TE.

CHAPTER 4

RESULTS AND DISCUSSION

In eukaryotic systems, site-directed mutagenesis of cyt c has supplied critical information on the role of specific residues in the hydrophobic and acidic sites, both of which are proposed to be involved in the interaction with PSI [47]. Whereas negative residues on the acidic part of the cyt c_{553} seem to be responsible for electrostatic interactions and complex formation with the positively charged PsaF subunit of PSI, the transfer of electrons from the cyt c_{553} to P700 in PSI could take place via the northern part of the protein [38, 47]. To study the importance of these acidic residues in the vicinity of the negative patches in the complex formation with PSI, a series of experiments were done in which mutagenic and native cyt c_{553} were used to reduce PSI. The rates at various pH and ionic strengths were also measured to infer the importance of interactions between the basic patch of PSI and the engineered acidic site in cyt c_{553}. The objective of this work was to investigate the effects of site-directed mutagenesis of *T. elongatus* cyt c_{553} on the electron transfer rate from cyt c_{553} to PSI. A thermophillic cyanobacterial system was chosen as the base for the source of cyt c_{553} because it is expected that it will have better thermal stability and possibly have a higher ET rate at higher temperatures.

4.1 Wild type cyt c_{553} and *T. elongatus* PSI

At the initiation of this study, the mutagenesis of cyt c_{533} was not completed. Therefore, experiments were started with the native cyt c_{553} (WT) and using the native PSI from *T. elongatus*.

4.1.1 Asc Titration

At sufficient concentrations, Asc is known to reduce PSI even in the absence of cyt c_{553}. Therefore, an initial experiment was done to determine what concentration of Asc was appropriate to avoid excess reduction of PSI by Asc. In all experiments, Asc was added before the mixtures were transferred to the reaction cuvettes to insure that the reduced forms of cyt c_{553} and PSI are present before the reaction is started by illuminating the samples. The experiments were done using two different detergents in the purification and stabilization of PSI, Triton and DM.

4.1.1.A Triton

The PSI reduction rates at different Asc concentration are displayed in Figure 10 for the case when PSI was purified and stabilized in Triton. Each rate presented here for reduction of PSI purified and suspended in Triton is the average of rates obtained simultaneously from three different probes. The error bars in all the figures represent standard deviations. The Asc concentration was varied between 0 and 32. For convenience, the concentrations of other substrates are listed in Table 4. Reduction of *T. elongatus* PSI by Asc shows a hyperbolic dependency on Asc concentration, increasing monotonically to a value of at approximately 1000 mmole O_2/hr/mg chl. From the figure, it can be seen that a concentration of 2mM Asc gives a relatively low PSI reduction rate; this concentration was therefore chosen as an appropriate Asc concentration for future experiments to avoid excess reduction of PSI by Asc.

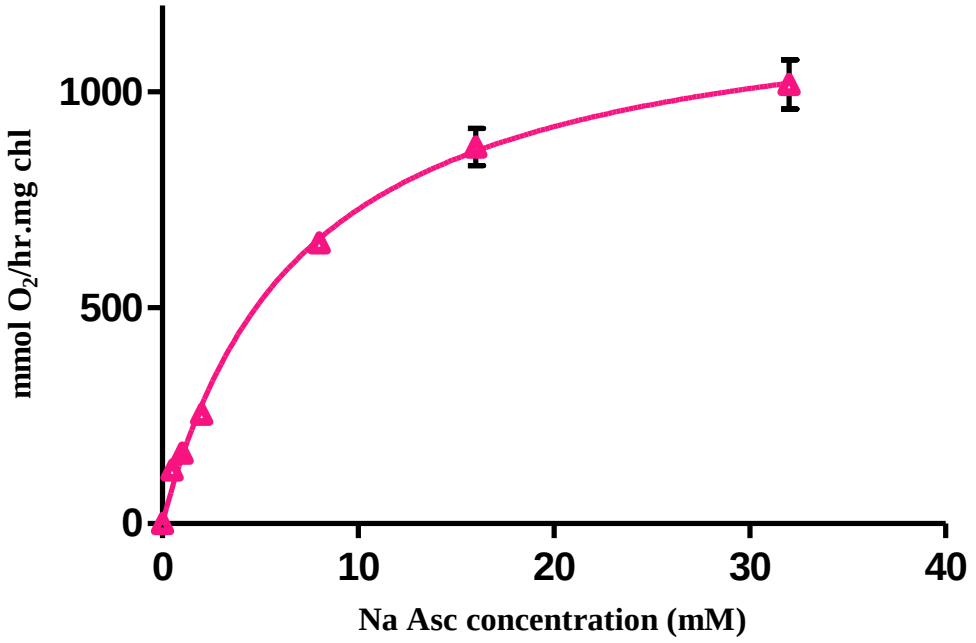

Figure 10: Influence of Asc concentration on the rate of reduction of C *T. elongatus* PSI purified and suspended in Triton

Table 4: Conditions of Asc influence on re-reduction of *T. elongatus* PSI purified and suspended in Triton.

Substrate	Concentration
MES buffer	10 mM
T.E. PSI	15 nM
WT T.E. cyt c_{553}	0
MV	167 μM
Ascorbic Acid	0-32 mM
Triton	0.02% (w/v)

4.1.1.B DM

The effect of Asc concentration on reduction of *T. elongatus* PSI purified and suspended in DM is depicted in Figure 11. The Asc concentration is varied between 0 and 16 mM by adding concentrated Asc solution to the buffer. The concentrations of other buffers are listed in Table 5. Each rate is the average of measured rates obtained from three probes as in the previous experiment. The results show a hyperbolic Asc concentration dependence of the reduction of PSI purified in DM as PSI purified in Triton, but its maximum value is 0.12 fold less (123 instead of 1018 mmole O_2/hr/mg chl). These results illustrate a trend in the experimental work conducted here; when Triton is used as a detergent in stabilizing the protein during purification and when resuspended in the reaction mixture, the re-reduction rate of PSI is higher.

4.1.2 Cyt titration with T. elongatus PSI

After determination of appropriate Asc concentration for the reaction which would not exceed PSI reduction, the dependence of the reduction of PSI on cyt c_{553} was investigated. The reaction mixture with *T. elongatus* PSI was titrated with WT *T. elongatus* cyt c_{553} at optimum Asc concentration (2mM). The results are shown in Figure 12. Each point is the average of measured data obtained simultaneously from four different probes. The conditions of the experiments are summarized in Table 6. As can be discerned from Figure 12, a low rate for PSI reduction was obtained in the absence of cyt c_{553} (see the left-most data point). This is caused by the reduction of PSI by Asc as discussed in the previous section. In the presence of cyt c_{553}, a faster PSI reduction rate is observed. The rate of electron transfer to PSI depends nonlinearly on the cyt c_{553} concentration. The saturating value for the molar ratio of cyt c_{553} will clearly be higher

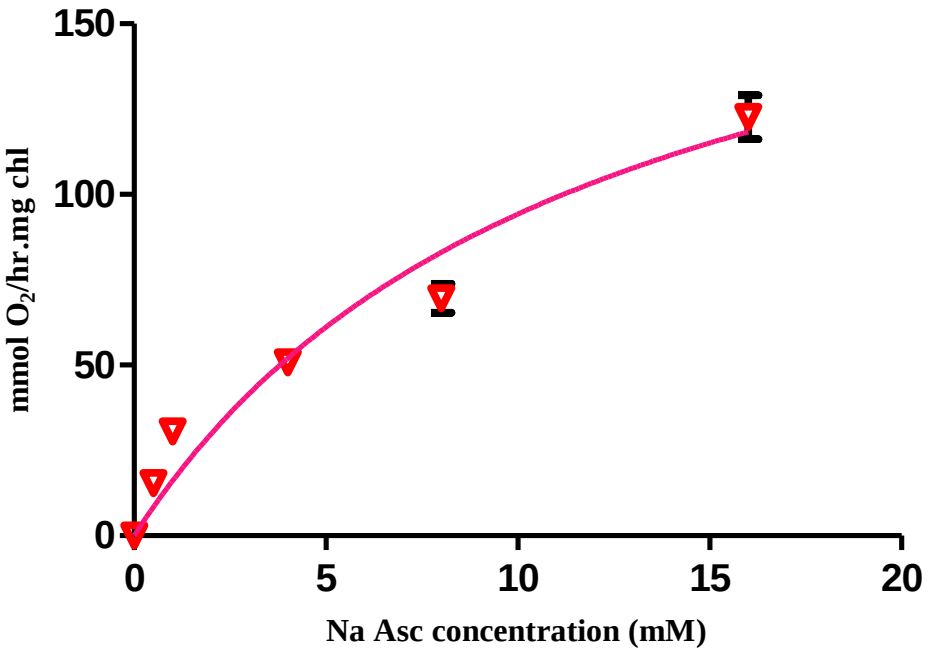

Figure 11: Influence of Asc concentration on the rate of reduction of *T. elongatus* PSI purified and suspended in DM

Table 5: Conditions of Asc influence on reduction o*f T. elongatus* PSI purified and suspended in DM.

Substrate	Concentration
MES buffer	10 mM
T.E PSI	15 nM
WT T.E cyt c_{553}	0
MV	167 μM
Ascorbic Acid	0-16 mM
DM	0.02% (w/v)

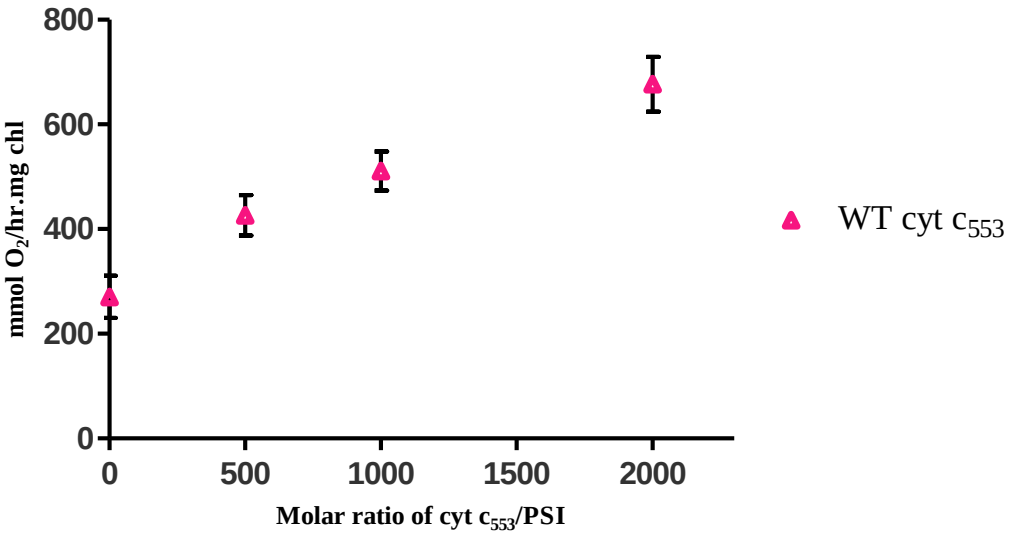

Figure 12: Influence of WT *T. elongatus* cyt c_{553} concentration on the rate of re-reduction of *T. elongatus* PSI.

Table 6: Conditions of WT *T. elongatus* cyt c_{553} titration with *T. elongatus* PSI.

Substrate	Concentration
MES buffer	10 mM
T.E PSI	5 nM
WT T.E cyt c_{553}	0-10,000 nM
MV	167 μM
Ascorbic Acid	2 mM
Triton	0.02% (w/v)

than the maximum tested of 2,000 moles cyt c_{553} per mol PSI, which corresponds to a cyt c_{553} concentration of 10,000 nM in this case.

4.1.3 pH Effect

The pH in the cyt c_{553} physiological environment is approximately 5 in the thylakoid lumen of photosynthetic organisms [57]. Acidic patches of cyt c_{553} which influence the electrostatic properties of the cyt c_{553} effect on electron transfer to PSI [57]. It is reasonable to believe that pH influences the structure, residues, and entities composing the acidic patches on cyt c_{553}, via protonation and deprotonation. Additionally, it seems reasonable that there would be a pH value where PSI and cyt c_{553} interactions would yield either an optimum or minimum PSI re-reduction rate. To examine the influence of pH on the reaction and electron transfer between WT cyt c_{553} and *T. elongatus* PSI, the pH in the solution was varied between approximately 5.45 and 8.68. The list of the buffers used for different pH is outlined in Table 7. The conditions of the experiment are listed in Table 8. The result is shown in Figure 13; each point is the average of four measured data points obtained from four probes simultaneously. Due to scatter in the data at the various pH values, it is difficult to determine if extrema exist. It appears that a small minimum may exist at a neutral pH, although the effect is small. This result indicates that there is no significant protenation or deprotenation of the WT cyt c_{553}.

4.1.4 Ionic Strength Effect

The effect of ionic strength has also been examined on the reduction of PSI by WT cyt c_{553}. The ionic strength is varied by adding small aliquots of concentrated salt (ammonium sulfate and sodium chloride) solutions. Compared to sodium chloride,

Table 7: Buffers used for different pH

Buffer (10 mM)	pH
Mono basic Sodium Phosphate and Citric acid	5
Bis-Tris	6
Tris	7
Tris	8
Bis-Tris Propane	9
CAPS	10

Table 8: Conditions of pH influence on re-reduction of *T. elongatus* PSI by WT *T. elongatus* cyt.

Substrate	Concentration
T.E PSI	5 nM
WT T.E cyt c_{553}	250
MV	167 μM
Ascorbic Acid	2 mM
Triton	0.02% (w/v)
pH	5.45-8.68

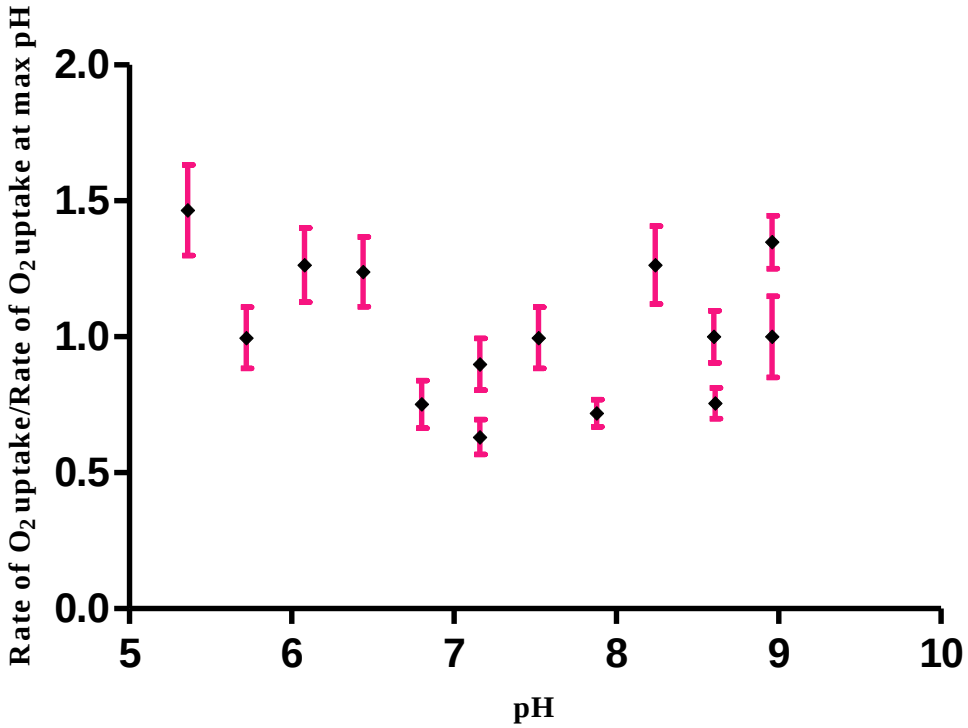

Figure 13: pH dependence of the rate of re-reduction of *T. elongatus* PSI by WT *T. elongatus* cyt c_{553}.

ammonium sulfate of same concentration is expected to exhibit a higher ionic strength influence on PSI reduction since it is divalent while sodium chloride is monovalent.

The ionic strength effect on the reduction of *T. elongatus* PSI by native *T. elongatus* cyt c_{553} is shown in Figure 14. Each point is the average of data obtained from four probes simultaneously. Ionic strength dependence of the rate of re-reduction of PSI by cyt c_{553} is examined using both ammonium sulfate and sodium chloride at pH 6.4. The ionic strength is varied between 0.03 mM and 500 mM for ammonium sulfate and between 0.03 mM and 100 mM for sodium chloride (Table 9).

Over the whole range of ionic strengths, the reduction of $P700^{ox}$ by cyt c_{553} (WT) is almost unchanged. The results indicate that there is not a strong ionic interaction between WT *T. elongatus* cyt c_{553} and *T. elongatus* PSI and the ionic strength does not have a strong effect on either the formation or the orientation of the protein-protein complex. This is consistent with the earlier results when the pH was varied and, taken together; these results indicate that the interactions between the native cytochrome and PSI are probably not electrostatic in nature.

4.1.5 Detergent Effect

The effects of different detergents during purification and when resuspending PSI were also studied because the literature and the previously shown data show that there is a significant effect on the reaction rate between cyt c_{553} and PSI.

A detergent has to be supplied to PSI/cyt c_{553} solutions to stabilize PSI to prevent the coagulation of its trimers. The detergents that were used in this study for PSI purification and resuspension in the reaction mixture were DM and Triton. To quantify the effect of detergents on the reduction of *T. elongatus* PSI, three cyt c_{553} titration experiments have

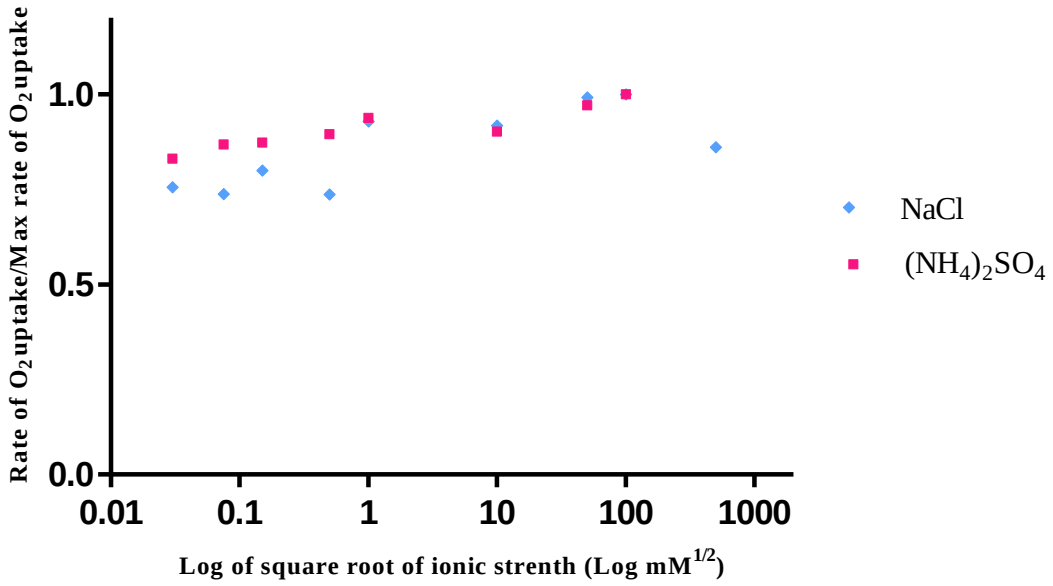

Figure 14: Ionic strength, WT *T. elongatus* cyt and *T. elongatus* PSI.

Table 9: Conditions of ionic strength influence on re-reduction of *T. elongatus* PSI by WT *T. elongatus* cyt c_{553}

Substrate	Concentration
MES buffer	10 mM
T.E PSI	5 nM
WT T.E cyt c_{553}	250 nM
MV	167 μM
Ascorbic Acid	2 mM
Triton	0.02% (w/v)

been conducted. In the first experiment PSI purified and resuspended in Triton is used, then, PSI purified and resuspended in DM, and in the last experiment PSI purified in DM, but resuspended in Triton is used. All three experiments were performed at pH 6.4 and the molar ratio of cyt c_{553} to PSI was varied between 0 to 1,000 (a concentration of 15 nM PSI) (Table 10). The results are shown in Figure 15. Each point is the average of data collected from four probes.

Figure 15 shows a hyperbolic concentration dependence on the cyt c_{553} concentration for all detergent combinations. Results indicate that the rate of PSI re-reduction is increased approximately 2.5 fold (from a mean of 284 to 695 mmole O_2/hr/mg Chl), for solutions containing PSI purified and resuspended in Triton, by increasing cyt c_{553} molar excess (with respect to 15 nM PSI) from 0 to 10,000. The PSI re-reduction rate is increased by approximately 3.6 fold (from a mean of 113 to 403 mmole O_2/hr/mg Chl) for solutions containing PSI purified and resuspended in DM, over the same range of cyt c_{553} molar excess. For PSI purified in DM, but re-suspended in Triton, there is approximately a 2-fold increase (from 309 to 615 mmole O_2/hr/mg Chl) in the reduction rate. PSI purified and resuspended in Triton shows a noticeably higher rate than other detergent combinations of PSI purification and suspension. It is possible that Triton renders the PSI docking site vulnerable to cyt c_{553} through a conformational change that takes place in the PSI structure when purified and resuspended in Triton. This conformation change can be explained by the interactions between regions of the cyt c_{553} with hydrophobic and hydrophilic regions of Triton leading to an increase in electron transfer to PSI via cyt c_{553}, increasing PSI reduction rate.

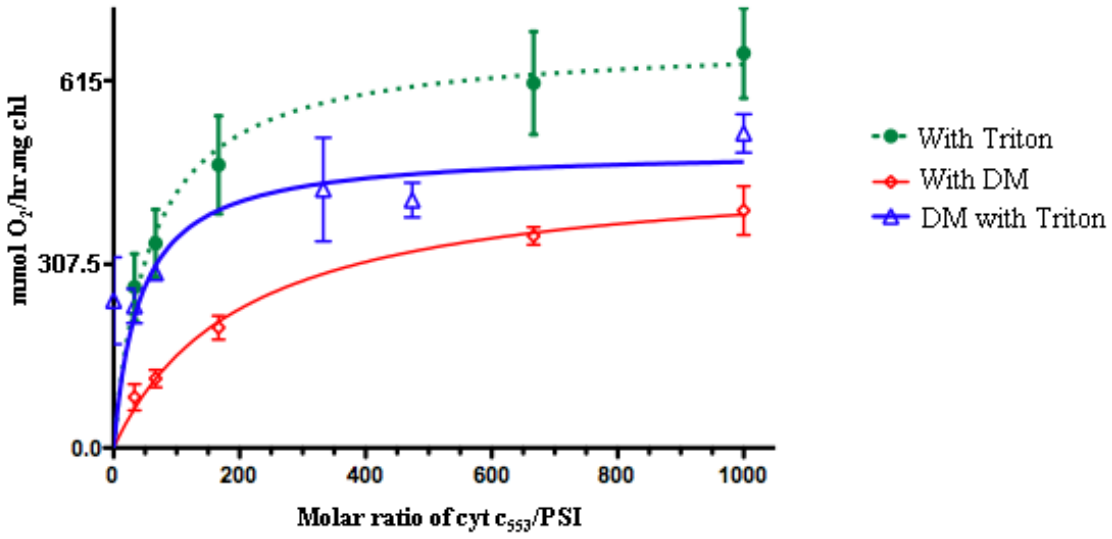

Figure 15: Detergent dependence of the re-reduction of *T. elongatus* PSI by WT *T. elongatus* cyt c_{553} (cyt c_{553} titration).

Table 10: Conditions of detergent influence on re-reduction of *T. elongatus* PSI by WT *T. elongatus* cyt c_{553} (cyt c_{553} titration)

Substrate	Concentration
MES buffer	10 mM
T.E PSI	15 nM
WT T.E cyt c_{553}	0-15,000 nM
MV	167 μM
Ascorbic Acid	2 mM
Triton /DM	0.02% (w/v)

4.2 Improved mutagenic cyt c_{553} and *T. elongatus* PSI

Chronologically, the previous experiments were conducted in parallel with efforts by others in the laboratory to develop an "improved" cyt c_{553} capable of interacting electrostatically with PSI. This was done by genetically engineering the cyt c_{553} gene from *T. elongatus* so that acidic residues similar to those in algal cyt c_{553} electron carriers would be translated and transcribed in cyt c_{553}. When the mutagenic cyt c_{553} was available, a set of experiments was conducted to examine the effect of the inserted residues in the mutagenic *T. elongatus* cyt c_{553} on its interaction with native *T. elongatus* PSI. The re-reduction rate of the native bacterial PSI by both the improved cyt c_{553} and the native cyt c_{553} were therefore compared for varying concentrations of the cyt c_{553}. The results are shown in Figure 16. Each point is the average of measured data obtained from four probes. The conditions of the experiments are summarized in Table 11.

This figure shows that the rate of electron transfer to PSI depends nonlinearly on the cyt c_{553} concentration for both the WT and the mutagenic cytochromes. The saturating molar ratio of cyt c_{553}/PSI for both cytochromes is higher than 2,000 (10,000 nM cyt c_{553}). Surprisingly, there is not much dependence on the concentration of c_{553} and the rate with the "unimproved" (WT) cytochrome was actually higher. While on the surface this result might appear to contradict the intent of the mutagenesis; however, it must be recalled that the native (*T. elongatus*) PSI was used in this experiment. The native PSI does not have the matching basic patches required for electrostatic interaction with the engineered cyt c_{553}. It is therefore likely that the inserted acidic patches from the algal cyt c_{553} degrade the cyt c_{553}:PSI binding which results in a lowered reaction rate between cyt c_{553} and PSI. Additionally, since the acidic side of the mutant is become more acidic by insertion of

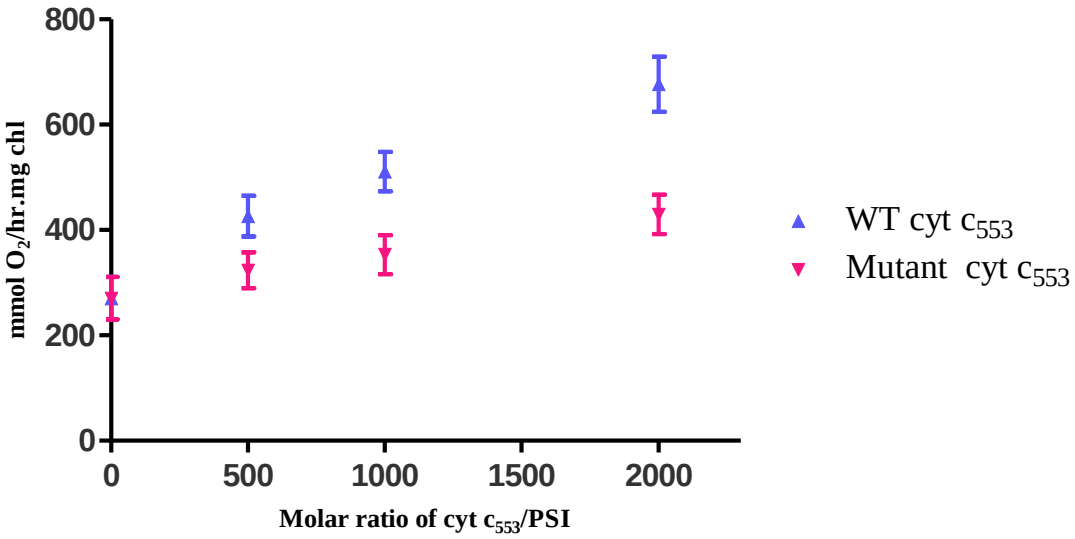

Figure 16: Comparison of the influence of WT and mutated *T. elongatus* cyt c_{553} concentration on the rate of re-reduction of *T. elongatus* PSI.

Table 11: Conditions of WT and mutated *T. elongatus* cyt c_{553} titration with *T. elongatus* PSI

Substrate	Concentration
MES buffer	10 mM
T.E PSI	5 nM
WT/mutated T.E cyt c_{553}	0-10,000 nM
MV	167 μM
Ascorbic Acid	2 mM
Triton	0.02% (w/v)

more acidic residues, it is possible that the mutated cyt c_{553} proteins aggregate due to the electrostatic interaction between themselves.

4.3 Improved cyt c_{553} and *C. reinhardtii* PSI

The previous experiment showed that pairing *T. elongatus* PSI with the improved cyt c_{553} resulted in a lower electron transfer rate to PSI than when *T. elongatus* PSI is paired with its WT cyt c_{553}. It was concluded that the improvements in the cyt could have actually inhibited binding with the bacterial PSI since it lacks the basic patches required for the interaction with the cyt c_{553}. One would expect that the presence of basic residues on the algal PSI would result in better binding between the mutant cyt c than the native cyt c.

4.3.1 WT and Improved Cyt Titrations

In order to investigate the effect of inserted acidic residues to *T. elongatus* cyt c_{553} on its electrostatic interaction with *C. reinhardtii* PSI (which, unlike *T. elongatus* PSI, does contain a basic patch) a series of experiments were performed in which a reaction mixture with *C. reinhardtii* PSI was titrated with both WT and the improved mutagenic cyt c_{553} (Figure 17). The conditions of the experiment are listed in Table 12. For these conditions, the experiments with the algal PSI indicated that there was no significant dependence on the protein (cyt c_{553}) concentration and the rates for both the mutated and WT cyt c_{553} were about the same with this PSI.

Another cyt c_{553} titration experiment was done in which WT cyt c_{553} was paired with *T. elongatus* PSI and the improved cyt c_{553} with *C. reinhardtii* PSI. In this case, each cytochrome was paired with PSI that had the appropriate matching binding site; that is, only hydrophobic interactions in the case of the WT cyt c_{553} and hydrophobic and

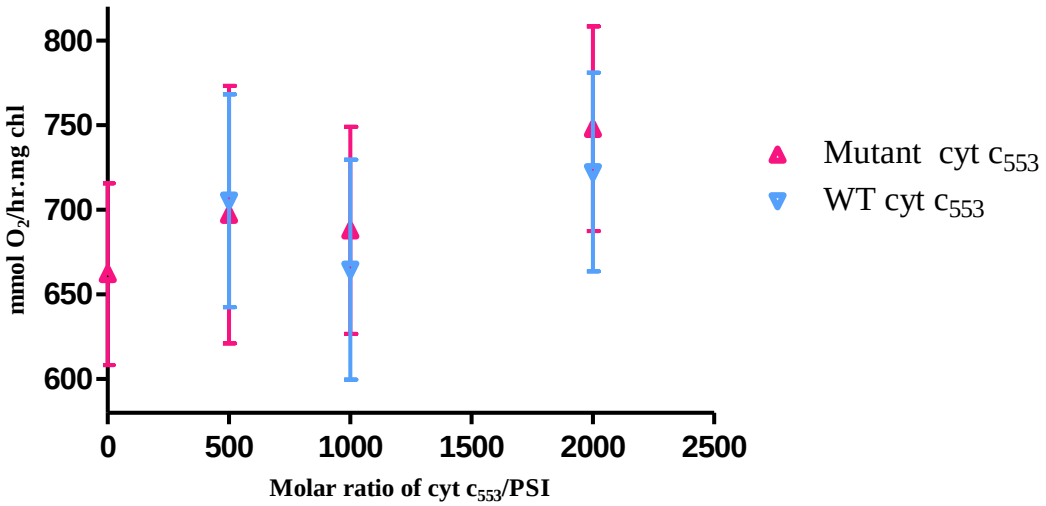

Figure 17: Comparison of the influence of WT and mutated *T. elongatus* cyt c_{553} concentration on rate of re-reduction of *C. reinhardtii* PSI.

Table 12: Conditions of WT and mutated *T. elongatus* cyt c_{553} titration with *C. reinhardtii* PSI

Substrate	Concentration
MES buffer	10 mM
C. *reinhardtii* PSI	5 nM
WT/mutated T.E cyt c_{553}	0-10,000 nM
MV	167 µM
Ascorbic Acid	2 mM
Triton	0.02% (w/v)

electrostatic in the case of the improved cyt c_{553}. The conditions of the experiments are listed in Table 13. As can be discerned from Figure 18, in the absence of cyt c_{553}, the rate of reduction of *C. reinhardtii* PSI by Asc is 2.77 fold higher than that of *T. elongatus* PSI. This implies that *C. reinhardtii* PSI is much more easily reduced than *T. elongatus* PSI resulting in a higher oxygen consumption rate. This indicates that the ascorbate concentration needed to minimize *C. reinhardtii* PSI re-reduction by ascorbate is lover than the concentration needed in the case of *T. elongatus* PSI. It was expected that the insertion of acidic residues to the acidic part of the *T. elongatus* cyt c_{553} facilitates the electrostatic interactions between acidic patches of cyt c_{553} and basic patches of PsaF subunit of *C. reinhardtii* PSI resulting in a higher electron transfer rate between the two partners. But, even though the rates obtained from pairing the improved cyt c_{553} with algal PSI were higher than that of pairing the WT cyt c_{553} with cyanobacterial PSI, it does not reflect the higher electrostatic interactions between the improved cyt c_{553} and PSI since the rate of reduction of algal PSI with Asc is much higher than that of cyanobacterial. Although the reaction of improved cyt c_{553} with *C. reinhardtii* PSI results in a higher rate, little (or for the improved cyt c_{553}, an inverse) dependence on the concentration of cyt c_{553} is observed. As the mutated cyt c_{553} concentration is increased the rate decreases faster which at high cyt c_{553} concentration the rate decrease to 0.6 fold of the rate in the absence of cyt c_{553}. It is not obvious why this inverse dependence exists and could be a result of poor data at the highest concentration of cyt c_{553}, where the inverse dependence is most exaggerated. The results do not show any cyt c_{553} concentration dependence of PSI re-reduction for improved cyt c_{553} with algal PSI. It is theorized that this might be because the light level was high increasing the PSI oxidation

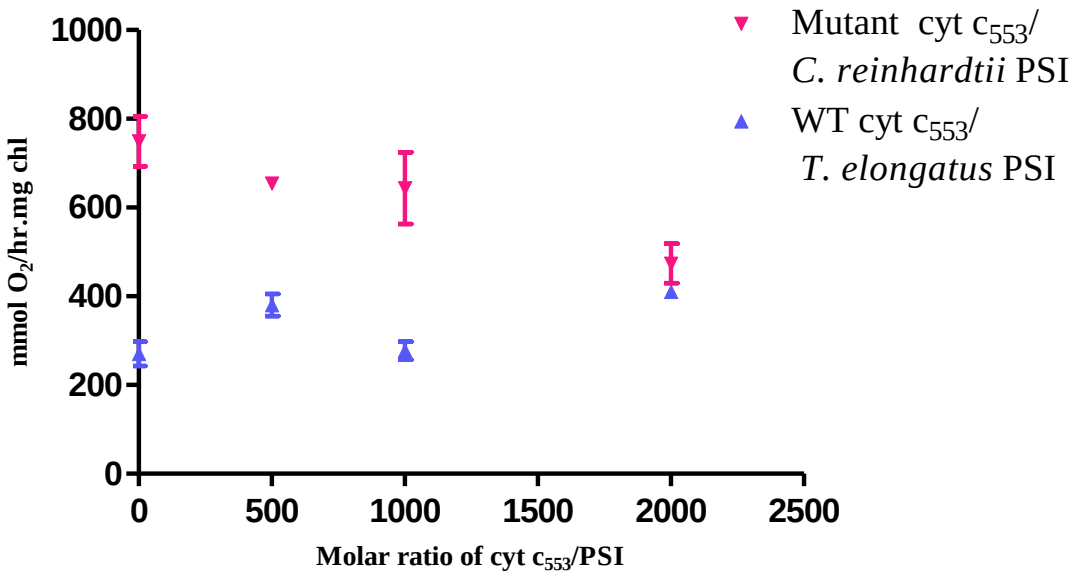

Figure 18: Comparison of the influence of WT and mutated *T. elongatus* cyt c_{553} concentration on rate of re-reduction of *T. elongatus* and *C. reinhardtii* PSI respectively.

Table 13: Conditions of WT and mutated *T. elongatus* cyt c_{553} titration with *C. reinhardtii* PSI and *T. elongatus* PSI, respectively.

Substrate	Concentration
MES buffer	10 mM
C. *reinhardtii*/ T.E PSI	5 nM
WT/mutated T.E cyt c_{553}	0-10,000 nM
MV	167 μM
Ascorbic Acid	2 mM
Triton	0.02% (w/v)

rate and could have caused an acceptor-side electron transfer "bottle-neck". At a sufficiently high concentration of cyt c, it is possible there is not enough MV to accept electrons from reduced PSI. In this case, the rate determining step in the reaction sequence could be the reduction of MV by PSI, not the reduction of PSI by cyt c_{553}. Therefore, the bottle-neck might be removed or decreased by increasing the MV concentration and lowering the light intensity. Before illuminating the samples, PSI is reduced by Asc and by illumination, after which the reaction starts with PSI entering the excited state. The excited PSI then is reduced by cyt c_{553}. With lower light the rate of excitation of PSI is lowered and the rate of re-reduction of PSI by cyt c_{553} decreases.

4.3.2 MV Titration

In the last experiment, the results did not show any cyt c_{553} concentration dependence of PSI re-reduction. It was theorized that this might be because the MV level was low decreasing the oxygen uptake rate. To find an appropriate MV concentration for the reaction, an experiment was conducted in which a mixture of *C. reinhardtii* PSI and improved *T. elongatus* cyt c_{553} was titrated with methyl viologen. The MV concentration was varied between 0 and 1,336 μM by adding small aliquots of a concentrated MV solution. The concentrations of the other reagents in the reaction mixture are outlined in Table 14. The points in Figure 19 are the average of two measured data points. The figure shows a hyperbolic MV concentration dependence of the reduction of *C. reinhardtii* PSI by the improved cyt c_{553}, which saturates at a rate of 230 mmole O_2/hr/mg Chl. The rate of PSI re-reduction is increased 1.52 fold (from 150 to 229 mmole O_2/hr/mg Chl) by doubling the MV concentration from167 to 334 μM.

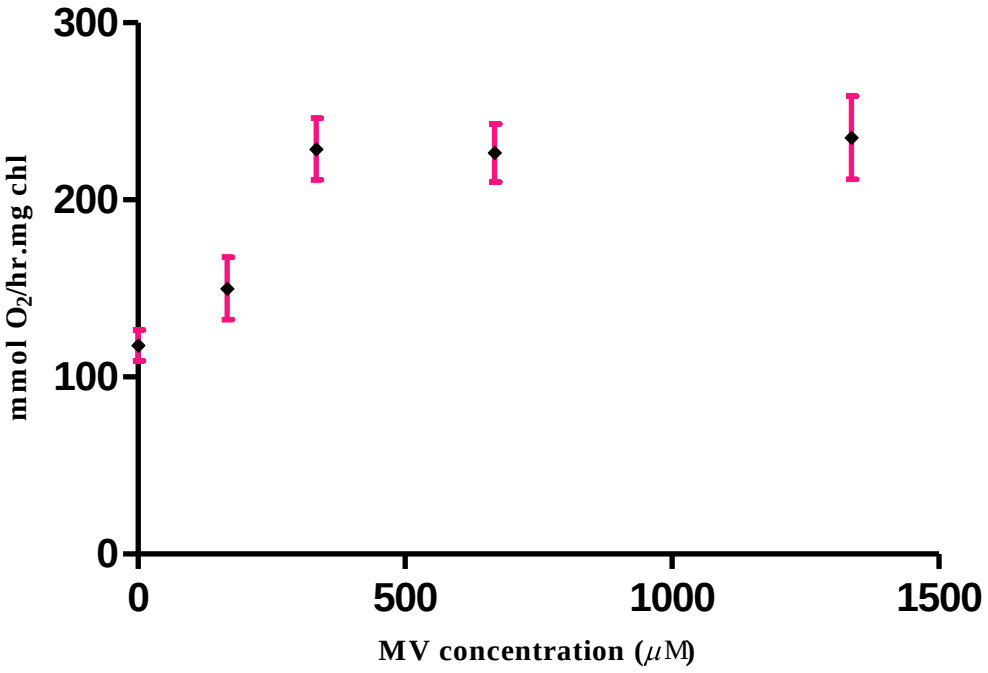

Figure 19: Influence of MV concentration on the rate of re-reduction of *C. reinhardtii* PSI by the mutant of *T. elongatus* cyt c_{553}.

Table 14: Conditions of MV influence on re-reduction of *C. reinhardtii* PSI by mutated *T. elongatus* cyt c_{553}

Substrate	Concentration
MES buffer	10 mM
C. *reinhardtii* PSI	5 nM
Mutated T.E cyt c_{553}	250
MV	0-1,336 μM

4.3.3 Improved Cyt Titration

The optimum MV concentration was found to be double the concentration used in the previous cyt c_{553} titration. To confirm that the decrease in rate at high concentration of improved cyt c_{553} was a result of an acceptor-side bottleneck (caused by a low concentration of MV) and a high re-reduction rate (caused by a high light intensity) an experiment similar to the previous one was performed at double MV concentration and less light. The influence of the mutant concentration on the rate of re-reduction of *C. reinhardtii* PSI is shown in Figure 20, which shows a common hyperbolic relationship, saturating at very high cyt c_{553}-to-PSI molar ratio(> 2000, corresponding to a cyt c_{553} concentration of 10,000 nM) (see Table 15). The data presented here reflect that the MV concentration was likely rate-determining in the previous experiment and a similar hyperbolic relationship which has been obtained for other protein-protein complexes [33, 36, 43, 49] can be obtained for improved cyt c_{553} titration at higher MV concentration. The conditions of the experiment are outlined in Table 15.

4.3.4 pH Effect

To examine the effect of inserted acidic residues to cyt c_{553} on the electrostatic interactions between the cytochrome and PSI, the effect of pH on the re-reduction of *C. reinhardtii* PSI by the improved cyt c_{553} was studied. As done previously, 10 mM buffers listed in Table 7 were used to vary the pH from approximately 5 to 10. The conditions that experiments are performed at are listed in Table 16. The results are shown in Figure 21 and each point is the average of two measured data points. It appears to be a more significant pH dependence for mutated cyt c_{553}/ *C. reinhardtii* PSI than for WT cyt c_{553}/ *T. elongatus* PSI and the data have less scatter.

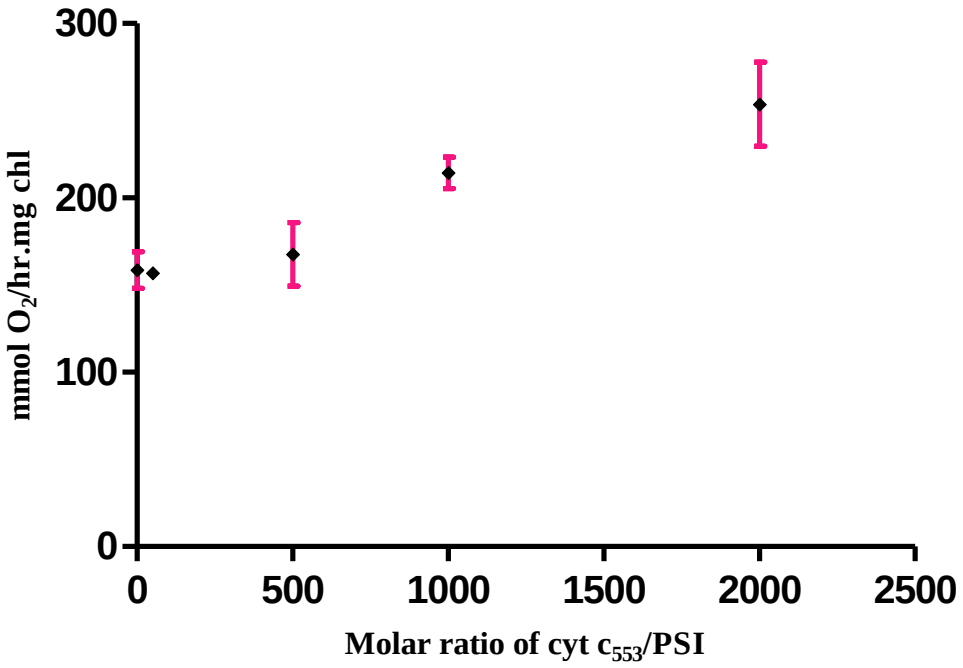

Figure 20: The influence of mutated *T. elongatus* cyt c_{553} concentration on rate of re-reduction of *C. reinhardtii* PSI.

Table 15: The mutated *T. elongatus* cyt c_{553} titration conditions with *C. reinhardtii* PSI

Substrate	Concentration
MES buffer	10 mM
C. *reinhardtii* PSI	5 nM
Mutated T.E cyt c_{553}	0-10,000 nM
MV	334 μM
Ascorbic Acid	2 mM
Triton	0.02% (w/v)

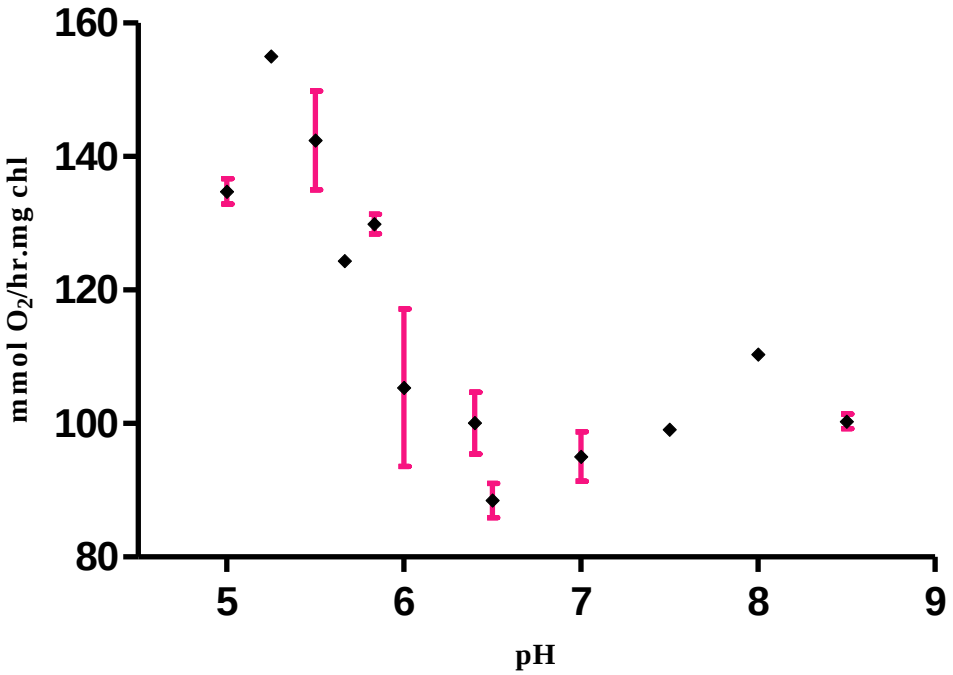

Figure 21: pH dependence of the rate of re-reduction of *C. reinhardtii* PSI by the mutant of *T. elongatus* cyt c_{553}.

Table 16: Conditions of pH influence on re-reduction of *C. reinhardtii* PSI by mutated *T. elongatus* cyt c_{553}

Substrate	Concentration
MES/HEPES/Tris buffer	10 mM
C. *reinhardtii* PSI	5 nM
Mutated T.E cyt c_{553}	250
MV	334 μM
Ascorbic Acid	2 mM
Triton	0.02% (w/v)

As can be discerned from the figure, at the lowest pH (pH 5) the rate is low and there is a maximum at pH around 5.25 followed by a decrease as pH is increased. This behavior is what is expected for cyt c_{553}:PSI pairings where the two proteins have the potential for electrostatic interactions; this reflects protonation and deprotonation, respectively, of residues important for the long range electrostatic attraction between the cyt c_{553} and PSI. At pH values below 5.25, the effect of low pH on PSI/cyt c_{553} is due to protonation of the local negative charges on the improved cyt c_{553}, making the cyt c_{553} inactive. Similary, at high pH rate decreases with the deprotonation of positive residues in PSI, again producing a situation unfavorable for electron transfer. The similar effect of pH on protein-protein interactions between plastocyanin and PSI has been observed [33, 36, 38, 43, 49].

The observations obtained by investigating the pH influence on the WT *T. elongates* cyt c_{553}/*T. elongates* PSI and mutated *T. elongates* cyt c_{553}/C. *reinhardtii* PSI reactions implies that the inserted patches to cyt c_{553} are essential for a proper contact between cyt c_{553} and PSI resulting in efficient $P700^{ox}$ reduction.

4.3.5 Ionic Strength Effect

Also, the effect of ionic strength on $P700^{ox}$ reduction was explored at pH 6.4 (the optimum pH, obtained from the last experiment) by gradually adding ammonium sulfate to the solution. The ionic strength is varied between 0.03 mM and 1M. The conditions of the experiment are listed in Table 17. Unlike with the *T. elongatus* PSI which lacks the basic patch to interact with the engineered acidic patch on the improved cyt, there is a much more obvious ionic strength dependence (Figure 22). The reduction of *C. reinhardtii* $P700^{ox}$ by the mutant of *T. elongatus* cyt c_{553} is biphasic with a maximum

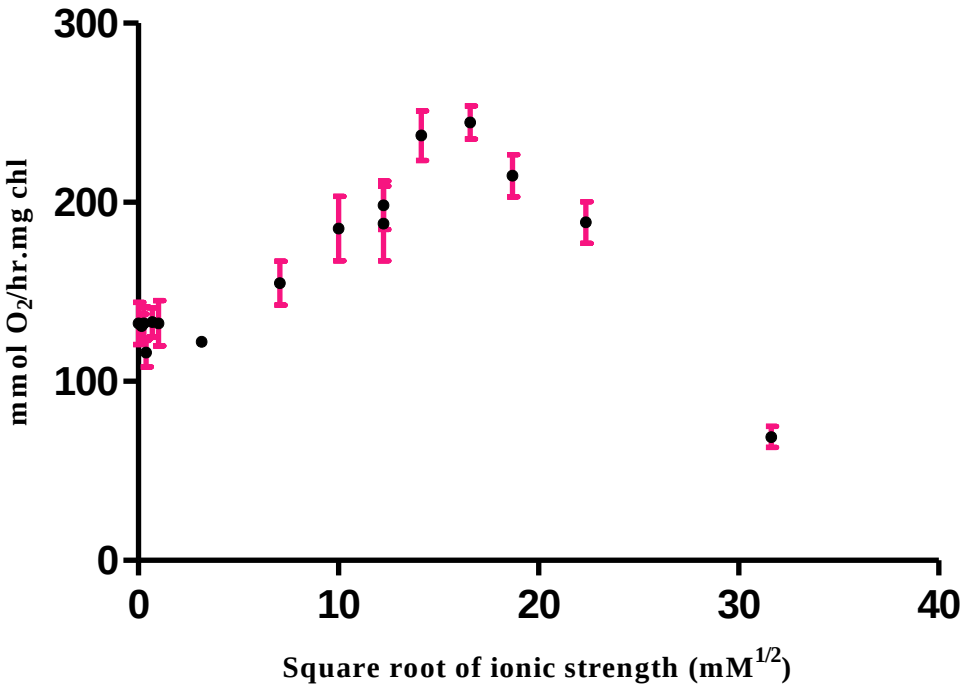

Figure 22: Ionic strength dependence of the re-reduction of *C. reinhardtii* PSI by the mutant of *T. elongatus* cyt c_{553}.

Table 17: Conditions of ionic strength influence on re-reduction of *C. reinhardtii* PSI by mutated *T. elongatus* cyt c_{553}

Substrate	Concentration
MES buffer	10 mM
C. *reinhardtii* PSI	5 nM
Mutated T.E cyt c_{553}	360 nM
MV	334 μM
Ascorbic Acid	2 mM
Triton	0.02% (w/v)

value obtained at approximately 275 mM ionic strength. A similar, bell-shaped, ionic strength dependency, where an intermediate ionic strength allows more favorable geometries, have been reported in literature for other photosynthetic protein-protein complexes, e.g. PSI/Pc, PSI/cyt c_6 and cyt b_6 f/cyt c_6 [27, 33, 34, 38, 43, 49]. It is seen that the observed rate varies in a complex way, increasing with ionic strength up to a maximum value at approximately 275 mM and then decreasing at higher salt concentrations. An upward sloping curve is expected since the negative charges on cyt c_{553} and positive charges on PSI are the determining factors in the electrostatic interaction between PSI and cyt c_{553}. A very low ionic strength, the electrostatic attractions between PSI and cyt c_{553} are strong, but their relative orientation of PSI and cyt c_{553} is not optimal for electron transfer. At intermediate ionic strength, some of these interactions are weakened and formation of an optimal complex is facilitated. This complex then dissociates at even higher salt concentrations. Thus, electrostatic interactions may facilitate the pre-orientation at long range of the two partners before they make physical contact and rearrange to form an optimal reaction complex.

CHAPTER 5

CONCLUSIONS

The resiprometric data from cyt titration experiments indicate that the introduction of acid patches from *C. reinhardtii* into *T. elongatus* cyt c_{553} allowed efficient binding and fast electron transfer between the cyanobacterial donor and *C. reinhardtii* PSI. The dependence of reaction rate on ionic strength suggests an effect due to molecular orientation within the intermediate complex. At optimum ionic strength, the electrostatic interaction may facilitate the pre-orintation at long range of the two partners before they make the optimal reaction complex. The pH dependence of the kinetics reflects the protonation and deprotonation of negative and positive charges on cyt c_{553} and PSI respictively important for the long-range electrostatic attraction between cyt c_{553} and PSI, i.e. interactions that govern the overall stability of the complex.

At the appropriate values for theses variables which do not cause a backup at the acceptor side of PSI, the PSI re-reduction rate by cyt c_{553} can be optimized. These conditions are approximately a pH of 5.5, an ionic strength of 275 mM, a relatively high MV concentration (334 μM), a lower light level, and a concentration of Asc that does not bypass cyt c_{553}, especially when *C. reinhardtii* PSI is used.

This work has shown that many variables need to be optimized and controlled to accurately compare re-reduction rates between different PSI:cyt c pairings. The logical next-step is to compare the rates between the improved and WT cyt c_{553} with *C. reinhardtii* PSI at the optimum pH and ionic strength values, lower light level, doubled MV concentration and lower Asc concentration. Also, the respirometric assay tends to be

difficult to perform and involves a measurement that is ultimately a composite rate of many reaction steps. Reaction rates for the same experiment vary significantly on different days, making it difficult to compare results between experiments occurring at different times. It was additionally observed that for lengthy experiments and experiments, in which extreme values of the experimental variables were used, the equipment appeared to act erratically and it was necessary to conduct many replicate experiments to obtain results with a sufficient degree of confidence. Flash photolysis is an experimental procedure commonly used to measure re-reduction kinetics and could possibly yield results with less variability. The rate of each step taking place before the electron transfer to PSI; formation of the complex and confirmation changes within the complex can be measured by flash photolysis. For a discussion of the use of flash photolysis to measure the kinetics of re-reduction, see the Appendix.

REFERENCES

1. *International Energy Outlook 2007* Energy information administration, May 2007. **Report #:DOE/EIA-0484(2007)**.
2. Kruse, O., et al., *Photosynthesis: a blueprint for solar energy capture and biohydrogen productio technologies.* Photochemistry and Photobiology, 2005. **4**: p. 957-969.
3. Hamilton, J., *A different kind of solar power.* Concordia university magazine, 2007. **Winter**.
4. Asada, Y. and J. Miyake, *Photobiological hydrogen production.* Journal of Bioscience and Bioengineering, 1999. **88**(1): p. 1-6.
5. Janssen, M.G.J., et al., *Biohydrogen 2002.* International Journal of Hydrogen Energy, 2002. **27**(11-12): p. 1123-1124.
6. Chen, C., C. Lin, and J. Chang, *Kinetics of hydrogen production with continuous anaerobic cultures utilizing sucrose as the limiting substrate.* Appl Microbiol Biotechnol, 2001(57): p. 56-64.
7. Mizunoa, O., et al., *Enhancement of hydrogen production from glucose by nitrogen gas sparging* Bioresource Technology 2000. **73**(1): p. 59-65
8. Badura, A., et al., *Light-driven water splitting for (bio-)hydrogen production: Photosystem 2 as the central part of a bioelectrochemical device.* Photochemistry and Photobiology, 2006. **82**(5): p. 1385–1390
9. Melis, A. and T. Happe, *Hydrogen production. Green algae as a source of energy*. Plant Physiol, 2001. **2001 November; 127(3): 740–748.**(3): p. 740–748.

10. Ihara, M., et al., *Photoinduced hydrogen production by direct electron transfer from photosystem I cross-linked with cytochrome c(3) to [NiFe]-hydrogenase.* Photochemistry and Photobiology, 2006. **82**(6): p. 1677-1685.

11. Jo, J.H., D.S. Lee, and J.M. Park, *Modeling and optimization of photosynthetic hydrogen gas production by green alga Chlamydomonas reinhardtii in sulfur-deprived circumstance.* Biotechnology Progress, 2006. **22**(2): p. 431-437.

12. Ihara , M., et al., *Light-driven hydrogen production by a hybrid complex of a [NiFe]-hydrogenase and the cyanobacterial Photosystem I.* Photochemistry and Photobiology, 2006. **82**(3): p. 676–682

13. Hallenbeck, P.C. and J.R. Benemann, *Biological hydrogen production; fundamentals and limiting processes.* International Journal of Hydrogen Energy, 2002. **27**(11-12): p. 1185-1193.

14. Kosourov, S., et al., *Sustained hydrogen production BY Chlamydomonas reinhardtii: Effects of culture parameters.* Biotechnology and Bioengineering, 2002. **78**(7): p. 731-740.

15. Fay, P. and C. Van Baalen, *The cyanobacteria*. 1 ed. Vol. 1. 1987, Amesterdam: Elsvier Science Publishers. 543.

16. Cournac, L., et al., *Sustained photoevolution of molecular hydrogen in a mutant of Synechocystis sp. strain PCC 6803 deficient in the type I NADPH-dehydrogenase complex* Journal of Bacteriology, 2004. **186**(6): p. 1737-1746.

17. Jansson, S., B. Andersen, and H. Scheller, *Nearest-neighbor analysis of higher-plant photosystem I holocomplex.* Plant Physiol, 1996. **112**: p. 409-420.

18. Ben-Shem, A., F. Frolow, and N. Nelson, *Crystal structure of plant photosystem I.* NATURE, 2003. **426**(6967): p. 630-635.

19. Fromme, P., et al., *Structure and function of photosystem I: interaction with its soluble electron carriers and external antenna systems.* FEBS Letters, 2003. **555**(1): p. 40-44.

20. Karapetyan, N.V., A.R. Holzwarth, and M. Rögner, *The photosystem I trimer of cyanobacteria: molecular organization, excitation dynamics and physiological significance.* FEBS Letters, 1999. **460**(3): p. 395-400.

21. Carmeli, I., et al., *Photovoltaic activity of Photosystem I-based self-assembled monolayer* J. Am. Chem. Soc., 2007. **129**(41): p. 12352 -12353,.

22. Santabarbara, S., P. Heathcote, and M. Evans, *Modelling of the electron transfer reactions in Photosystem I by electron tunneling theory: The phylloquinones bound to the PsaA and PsaB reaction centre subunits of PSI are almost isoenergetic to the iron-sulfur cluster Fx.* Biochimica et Biophysica Acta, 2005. **1708**: p. 283-310.

23. Ratajczak, R., R. Mitchell, and H. Wolfgang, *Properties of the oxidizing site of Photosystem I.* Biochimica et Biophysica Acta (BBA) - Bioenergetics, 1988. **933**(2): p. 306-318.

24. Hervás, M., et al., *Electron transfer reactions in both the oxidizing and reducing sites of photosystem I : A laser flash absorption spectroscopy study.* Bioelectrochemistry and Bioenergetics, 1992. **28**(1-2): p. 205-212.

25. Webber, A.N. and W. Lubitz, *P700: the primary electron donor of photosystem I.* Biochimica et Biophysica Acta (BBA) - Bioenergetics, 2001. **1507**(1-3): p. 61-79.

26. Whitmarsh, J. and Govindjee, *The photosynthesis*. Concepts in photobiology: Photosynthesis and Photomorphogenesis, ed. G. Singhal, et al. Vol. 1. 1999, New Dehli: Narosa Pub;ishers. 1019.

27. Hervas, M., et al., *Laser-flash kinetic analysis of the fast electron transfer from plastocyanin and cytochrome c(5 to photosystem I. Experimental evidence on the evolution of the reaction mechanism.* Biochemistry, 1995. **34**: p. 11321-1 1326

28. Wood, P.M., *Rate of electron transfer between plastocyanin, cytochrome f, related proteins and artificial redox reagents in solution.* Biochimica et Biophysica Acta (BBA) - Bioenergetics, 1974. **357**(3): p. 370-379.

29. Baymann, F., et al., *Rapid electron transfer to photosystem I and unusual spectral features of cytochrome c_6 in Synechococcus sp. PCC 7002 in vivo.* Biochemistry, 2001. **40**(35): p. 10570 -10577.

30. Hervas, M., et al., *Cyanobacterial photosystem I lacks specificity in its interaction with cytochrome c(6) electron donors.* PHOTOSYNTHESIS RESEARCH, 2005. **83**(3): p. 329-333.

31. Petrouleas, V., et al., *A Mössbauer study of the CYT b6/f - Rieske complex.* Journal of Inorganic Biochemistry, 1995. **59**(2-3): p. 546-546.

32. Sujak, A., F. Drepper, and W. Haehnel, *Spectroscopic studies on electron transfer between plastocyanin and cytochrome b6f complex.* Journal of Photochemistry and Photobiology B: Biology, 2004. **74**(2-3): p. 135-143.

33. Sigfridsson, K., *Ionic strength and pH dependence of the reaction between plastocyanin and Photosystem I. Evidence of a rate-limiting conformational change.* Photosynthesis Research, 1997. **54**: p. 143–153.

34. Hippler, et al., *Insertion of the N-terminal part of PsaF from Chlamydomonas reinhardtii into photosystem I from Synechococcus elongatus enables efficient binding of algal plastocyanin and cytochrome c_6.* THE JOURNAL OF BIOLOGICAL CHEMISTRY, 1999. **247**(February 12,): p. 4180–4188.

35. Nordling, M., et al., *Flash-photolysis studies of the electron transfer from genetically modified spinach plastocyanin to photosystem I.* FEBS Letters, 1991. **291**(2): p. 327-330.

36. Sigfridsson, K., et al., *Spectroscopic and kinetic characterization of the spinach plastocyanin mutant Tyr83-His: a histidine residue with a high p K value.* Biochimica et Biophysica Acta, 1995. **1228**: p. 28-36.

37. Sigfridsson, K., *Plastocyanin, an electron-transfer protein.* Photosynthesis Research, 1998. **57**: p. 1-28.

38. Hope, A., *Electron transfers amongst cytochrome f, plastocyanin and photosystem I : kinetics and mechanisms.* Biochimica et Biophysica Acta, 2000. **1456** p. 5-26.

39. Zhang, L., et al., *Copper-mediated regulation of cytochrome c553 and plastocyanin in the cyanobacterium Synechocystis 6803.* J. Biol. Chem., 1992. **267**(27): p. 19054-19059.

40. Hippler, M., et al., *Fast electron transfer from cytochrome c6 and plastocyanin to photosystem I of*

Chlamydomonas reinhardtii requires PsaF. Biochemistry, 1997. **36**: p. 6343-6349.

41. Sommer, F., et al., *Identification of precise electrostatic recognition sites between cytochrome c6 and the photosystem I subunit PsaF using mass spectrometry.* J. Biol. Chem., 2006. **281**(46): p. 35097-35103.

42. Sommer, F., et al., *The hydrophobic recognition site formed by residues PsaA-Trp651 and PsaB-Trp627 of photosystem I in Chlamydomonas reinhardtii confers distinct selectivity for binding of plastocyanin and cytochrome c6*.* THE JOURNAL OF BIOLOGICAL CHEMISTRY, 2004. **279**(My 7): p. 20009–20017.

43. Sigfridsson, K., S. Young, and O. Hansson, *Electron transfer between spinach plastocyanin mutants and photosystem 1.* Eur. J. Biochem. , 1997. **245**: p. 805-812.

44. Iwuchukwu, I., et al., *Self-assembled photosynthetic nanoparticle for cell-free hydrogen production* Submitted for publication, 2008.

45. Hippler, M., et al., *Light-Induced Charge Separation between Plastocyanin and the Iron-Sulfur Clusters FAand FBin the Complex of Plastocyanin and Photosystem I.* Archives of Biochemistry and Biophysics, 1996. **330**(2): p. 414-418.

46. Blankenship, R., *Molecular mechanisms of photosynthesis*, ed. B. Science. Vol. 1. 2002, London: Blackwell Science.

47. Cerda, B., et al., *Site-directed mutagenesis of cytochrome c6 from Synechocystis sp. PCC 6803.* THE JOURNAL OF BIOLOGICAL CHEMISTRY, 1999. **274, No. 19, Issue of May 7, pp. ,** (May 7): p. 13292–13297.

48. Hervás, M., et al., *Laser flash kinetic analysis of Synechocystis PCC 6803 cytochrome c6 and plastocyanin oxidation by Photosystem I.* Biochimica et Biophysica Acta (BBA) - Bioenergetics, 1994. **1184**(2-3): p. 235-241.

49. Sigfridsson, K., et al., *A comparative flash-photolysis study of electron transfer from pea and spinach plastocyanins to spinach Photosystem 1. A reaction involving a rate-limiting conformational change.* Photosynthesis Research, 1996. **50**: p. 11-21.

50. Incorporated, Y., *YSI model 5300 biological oxygen monitor instruction manual*.

51. Saha, S., L. Uma, and G. Subramanian, *An improved method for marine cyanobacterial DNA isolation.* World journal of microbililogy & biotechnology, 2005. **21** (6-7): p. 877-881.

52. Schägger, H. and G. von Jagow, *Tricine-sodium dodecyl sulfate-polyacrylamide gel electrophoresis for the separation of proteins in the range from 1 to 100 kDa.* Analytical Biochemistry, 1987. **166**(2): p. 368-379.

53. *pET system manual.* Novagen, 1999. **8th edition**.

54. *Site-directed mutagenesis kit*.

55. Schatz, G. and H. Witt, *Extraction and characterization of oxygen-evolving photosystem-II complexes from a thermophilic cayanobacteriun Synechococcus spec.* Photobioch Photobiop () vol. 7 (1) pp. , 1984. **7**(1): p. 1-14.

56. Fromme, P. and H. Witt, *Improved isolation and crystallization of Photosystem I for structural analysis.* Biochim. Biophys. Acta-Bioenerg. () vol. 1365 (1-2) pp. 175-184, 1998. **1365**(1-2): p. 175-184

57. Ullmann, G., et al., *Comparison of the physiologically equivalent proteins cytochrome c6 and plastocyanin on the basis of their electrostatic potentials. Tryptophan 63 in cytochrome c6 may be isofunctional with tyrosine 83 in plastocyanin.* . Biochemistry, 1997. **36**(1): p. 16187-16196.

58. MATHIS, P., I. IKEGAMI, and P. SETIF, *Nanosecond flash studies of the absorption spectrum of the Photosystem I primary acceptor A_o.* Photosynthesis Research, 1988. **16**: p. 203-210.

59. Drepper, F., et al., *Binding dynamics and electron transfer between plastocyanin and photosystem I.* Biochemistry 1996. **35**: p. 1282-1295.

60. Haehnel, W., A. Propper, and H. Krause, *Evidence for complexed plastocyanin as the immediate electron donor of P-700.* Biochimica et Biophysica Acta (BBA) - Bioenergetics, 1980. **593**(2): p. 384-399.

61. Bottin, H. and P. Mathis, *Interaction of plastocyanin with thephotosystem I reaction center: A kinetic*

study by flash absorption spectroscopy Biochemistry 1985. **24**: p. 6453-6460.

62. Haehnel, W., V. Hesse, and A. Pröpper, *Electron transfer from plastocyanin to P700 : Function of a subunit of photosystem I reaction center.* FEBS Letters, 1980. **111**(1): p. 79-82.

63. Sigfridsson, K., S. Young, and O. Hansson, *Structural dynamics in the plastocyanin-photosystem 1 electron-transfer complex as revealed by mutant studies.* Biochemistry, 1996. **35**(4): p. 1249 -1257.

64. Hargrove, M., *A Flash Photolysis Method to Characterize Hexacoordinate Hemoglobin Kinetics.* Biophysical Journal, 2000. **29**: p. 2733–2738.

65. Hoganson, C.W., P.A. Casey, and O. Hansson, *Flash photolysis studies of manganese-depleted Photosystem II: evidence for binding of Mn2+ and other transition metal ions.* Biochimica et Biophysica Acta (BBA) - Bioenergetics, 1991. **1057**(3): p. 399-406.

APPENDIX

Flash Photolysis Studies

Although a lot of work has been done to improve the interaction between Pc and P700 in PSI in a wide variety of organisms, not much work has been done to achieve high electron transfer rates from cyt c_{553} to PSI. This thesis addressed the interaction between the electron donor, cyt_{533}, and the electron acceptor, P700, in the cyanobacterium *T. elongatus*. There is little literature that deals specifically with this system; however, there were several studies in the 1990's that developed models for the kinetics of P700 re-reduction by plastocyanin found in algae, higher plants, and some cyanobacteria. As a result of the similarity in function between plastocyanin and cyt_{553} in reducing P700, the results of these earlier kinetic studies with plastocyanin are used as the electron donor to develop models for the system discussed here, which uses cyt c_{553}. In addition, any chemical reaction system with the same reaction mechanism ($A^o + B^r \leftrightarrow A^o....B^r \leftrightarrow A^o.B^r \rightarrow A^r.B^o$) will result in the same rate expressions. Therefore in this work, a study by Hargrove to derive, by analogy, methods for determining the rate constants for P700 re-reduction from experimental measurements is used.

The reaction mechanism of electron transfer from cyt c_{553} to P700 can be studied by flash-photolysis. Flash-excitation of a mixture of PSI particles and cyt c_{553} results in an instantaneous absorption increase at 830 nm due to photo-oxidation of PSI followed by a slower absorption decrease to the baseline in an exponential manner due to reduction of oxidized PSI by cyt c_{553} [36, 43]. This electron transfer reaction between reduced cyt c_{553} and PSI can be investigated with time-resolved absorption measurements at 830 nm.

As it can be discerned from Figure 23, there is a big peak at 700 nm, but it has a high background from other chlorophylls in PSI. The small peak at 830 nm is unique to pick P700 only since it has no back ground from other PSI chlorophylls [58].

The analysis for the determination of the kinetic constants for the electron transfer reactions between cyt c_{553} and P700, the reaction center of PSI, can be made in terms of the following model:

$$\text{cyt } c_{553}^{\,r} + \text{P700}^{\,o} \underset{k_{off}}{\overset{k_{on}}{\rightleftharpoons}} \text{cyt } c_{553}^{\,r} \text{....} P_{700}^{\,o} \underset{k_c}{\overset{k_d}{\rightleftharpoons}} \text{cyt } c_{553}^{\,r} . P_{700}^{\,o} \xrightarrow{k_{et}} \text{cyt } c_{553}^{\,o} . P_{700}^{\,r}, \tag{5}$$

where cyt $c_{553}^{\,r}$ = reduced cyt c_{553}
cyt $c_{553}^{\,o}$ = oxidized cyt c_{553}
$P700^r$ = reduced P700
$P700^o$ = oxidized P700

It is known that this scheme can be used at high concentrations of cyt c_{553}. The applicability of this model will be addressed in the next chapter. For this reaction the system of ordinary differential equations can be written as follows:

$$\frac{d[P_{700}^{\,o}]}{dt} = -[\text{cyt } c_{553}^{\,r}][P_{700}^{\,o}]k_{on} + [\text{cyt } c_{553}^{\,r} \text{....} P_{700}^{\,o}]k_{off} \tag{6}$$

$$\frac{d[\text{cyt } c_{553}^{\,r} \text{....} P_{700}^{\,o}]}{dt} = [\text{cyt } c_{553}^{\,r}][P_{700}^{\,o}]k_{on} - [\text{cyt } c_{553}^{\,r} \text{....} P_{700}^{\,ox}](k_{off} + k_d) + [\text{cyt } c_{553}^{\,r} . P_{700}^{\,o}]k_c \tag{7}$$

$$\frac{d[\text{cyt } c_{553}^{\,r} . P_{700}^{\,o}]}{dt} = -[\text{cyt } c_{553}^{\,r} . P_{700}^{\,o}](k_{et} + k_c) + [\text{cyt } c_{553}^{\,r} \text{....} P_{700}^{\,o}]k_d \tag{8}$$

$$\frac{d[\text{cyt } c_{553}^{\,o} . P_{700}^{\,r}]}{dt} = [\text{cyt } c_{553}^{\,r} . P_{700}^{\,o}]k_{et} \tag{9}$$

An analytical solution for this system of ODEs exists when the reaction starts with cyt c_{553} in large excess over P700, where the possible inhibition by oxidized cyt c_{553} can be neglected [43, 59]. It has been experimentally observed that three kinetic components or "phases" can be resolved for the reduction of P700 by cyt c_{553} [27, 35]. It is generally observed that the two fastest phases involve the formation of a cyt $c_{553}^{\,red}$.

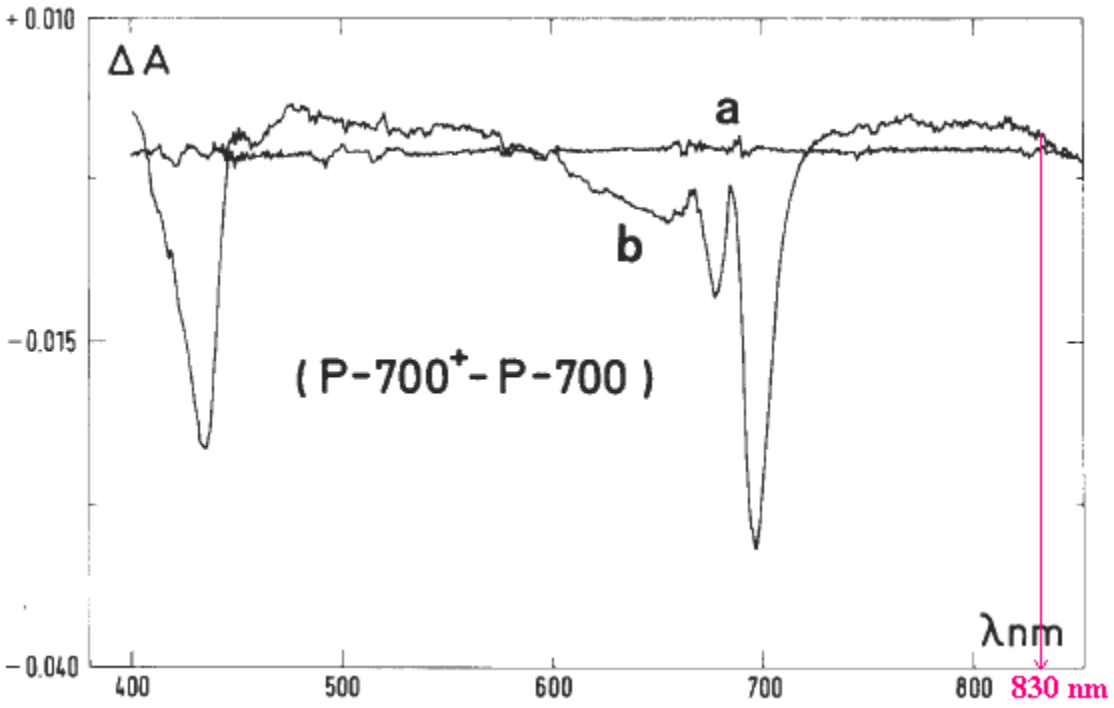

Figure 23: Difference spectra obtained with P700 enriched PSI particles. Curve b is a steady state difference spectrum between an oxidized and a reduced sample; curve a is a base-line [58].

$P700^{ox}$ complex and the electron-transfer from cyt c_{553} to P700.

The decay lifetime of the fastest phase is 10-20 μs and that of the second fastest is about 200 μs [40, 60-62]. The experimentally observed third phase arises from the reduction of cyt c_{553}^{ox} by Asc [33, 35].

All three rate constants for the electron transfer and the conformational change within the complex, k_{et}, k_c and k_d, can be calculated by fitting three exponentials into the signals obtained from the absorption change at 830 nm (Figure 24); usually this is done with a nonlinear least-squares curve-fitting algorithm [43]. Acquisition of the transient absorption signals and fitting of the signals to a sum of exponentials will be described later. To provide a better understanding of the reaction mechanism of the interaction of

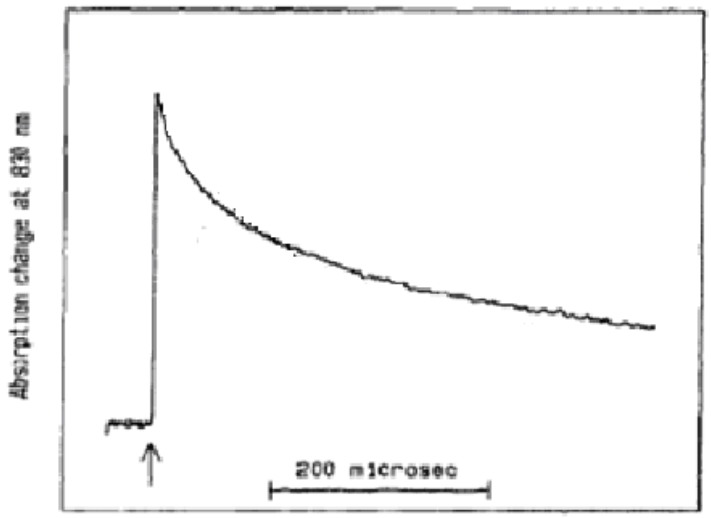

Figure 24: Flash-induced absorption transient at 830 nm of PSI particles with plastocyanin [35-37].

cyt c_{553} and PSI, the previous studying the kinetics of the electron transfer from Pc and cyt c_{553} to PSI is discussed in this section.

Kinetic Models

For modeling the ET between Pc or cyt c_{553} to PSI, three or more steps can be discerned. The number of steps in the mechanism depend on the involvement of one or more conformational changes or rearrangements within the complex before electron transfer can take place [43]. Regardless of how many conformational changes before electron transfer to PSI are considered, good curve-fits to the experimental data can be obtained if the model function consists of a sum of three decaying exponentials [36]. The amplitudes and apparent decay lifetimes of the exponentials will be denoted by A_i and τ_i, where i = 1-3. A first-order reaction involving a reactant C can be described as follows:

$$C \xrightarrow{\lambda} B \qquad (10)$$

$$\frac{d[B]}{dt} = -\frac{d[C]}{dt} = -\lambda[C] \tag{11}$$

The solution to Equation (11) is below, where [C] is the quantity and the rate constant λ is a positive number often called the decay constant.

$$\frac{[C(t)]}{[C_0]} = \frac{1}{e^{\lambda t}} \tag{12}$$

$$[C(t)] = [C_0]e^{-\lambda t} \tag{13}$$

$$\tau = \frac{1}{\lambda}\ , [C(t)] = [C_0]e^{-t/\tau} \tag{14}$$

As seen in Equation 14, the parameter τ is the multiplicative inverse of the decay constant, λ; it is often called the decay lifetime. Figure 25 show the time dependence of $[C(t)]/[C_0]$ with different decay lifetimes.

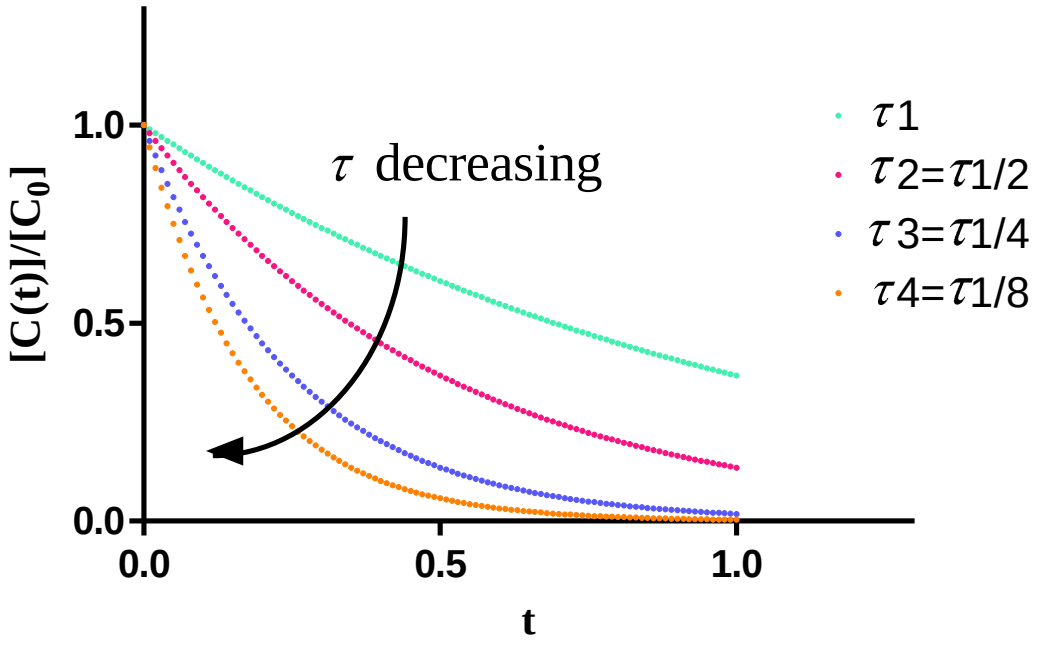

Figure 25: Dependency of exponential with one decay phase on life time.

From a curve-fitting analysis of the data from the absorption change at 830 nm, it has been shown that the third amplitude (A_3) of the slowest (decay lifetime on the order of milliseconds) component is constant at about 20% of the total initial amplitude when Pc is in the large excess over P700. In the experimental work done to confirm the validity of these models, sodium ascorbate was always present in the reaction medium to reduce Pc before the reaction starts by illumination, and methylviologen to prevent a back reaction between the photoreduced PSI electron acceptors and $P700^{ox}$ [49]. In the absence of Pc, a rapid absorbance increase from $P700^{ox}$ is followed by a slow decay due to its reduction by ascorbate. After Pc addition, the signal decays faster and with a more complex behavior. About 80% of the signal shows a biphasic decay, while the remaining fraction is assigned to oxidized Pc that is reduced by ascorbate [49].

The absorption signal at 830 nm has contribution from both $P700^{ox}$ and Pc^{ox} [35]. Since the absorption coefficient of Pc^{ox} at 830 nm is 18% of that of $P700^{ox}$ (absorption coefficients, 5500 $M^{-1} cm^{-1}$ for $P700^{ox}$ and 1000 $M^{-1} cm^{-1}$ for Pc^{ox}), it is reasonable to ascribe this component to the reduction of Pc^{ox} by ascorbate [35, 36, 49, 63]. The first two components are ascribed to the decay kinetics of $P700^{ox}$ (the two fast phases).

The following model (15) can be considered as the simplest model in which the intracomplex ET is preceded only by the complex-formation step determined by the rate constants k_{on} and k_{off}. This reaction scheme has been used by Nordling et al. [35] for ET between Pc and P700 and by the similar reaction for analyzing ligand binding to hemoglobin by Hargrove [64].

$$Pc^{r} + P_{700}{}^{o} \underset{k_{off}}{\overset{k_{on}}{\rightleftharpoons}} Pc^{r}.P_{700}{}^{o} \xrightarrow{k_{et}} Pc^{o}.P_{700}{}^{r} \qquad (15)$$

where Pc^{r} = reduced Pc

Pc^o = oxidized Pc

At low Pc concentration, this scheme results in an increase in the amplitude of the third phase (A_3) with a decrease in the Pc concentration which is expected to remain constant (at 18% of the total initial amplitude). This means that an additional, third, component appears in the P700 ^{ox} decay kinetics at low Pc concentrations. The addition of another P700 reducing component was found to be unreliable since it results in four decaying exponentials [36]. Therefore this scheme could not account for the observations in previous work if Pc was not in excess over PSI.

Even with the above shortcomings, this scheme has been in early work used for analysis of PSI reduction by Pc and similar reactions when the reducing component is in a large excess over the reduced component and biexponential reduction kinetics of P700 have been obtained [35, 64]. Later, however, this model was discarded as too simple by Sigfridsson et al. [36, 63]. They claimed that the amplitude of the second phase would approach zero which results in a monoexponential decay of $P700^{ox}$. The more complicated kinetic model suggested by Sigfridsson is as follows:

$$Pc^r + P_{700}{}^o \underset{k_{off}}{\overset{k_{on}}{\rightleftarrows}} Pc^r .... P_{700}{}^o \underset{k_c}{\overset{k_d}{\rightleftarrows}} Pc^r . P_{700}{}^o \xrightarrow{k_{et}} Pc^o . P_{700}{}^r \quad , \tag{16}$$

and, by analogy, for cyt c_{553} as an electron donor to P700:

$$\text{cyt } c_{553}{}^r + P700^o \underset{k_{off}}{\overset{k_{on}}{\rightleftarrows}} \text{cyt } c_{553}{}^r .... P_{700}{}^o \underset{k_c}{\overset{k_d}{\rightleftarrows}} \text{cyt } c_{553}{}^r . P_{700}{}^o \xrightarrow{k_{et}} \text{cyt } c_{553}{}^o . P_{700}{}^r \quad . \tag{17}$$

Figure 26 shows the long-range electrostatic interactions between basic patches on PsaF and acidic patches on the donor, which in this case is cyt c_{553}. The interaction of cytochrome c_{553} with PsaF is designated as “Docking Site 1”. Electron transfer occurs at

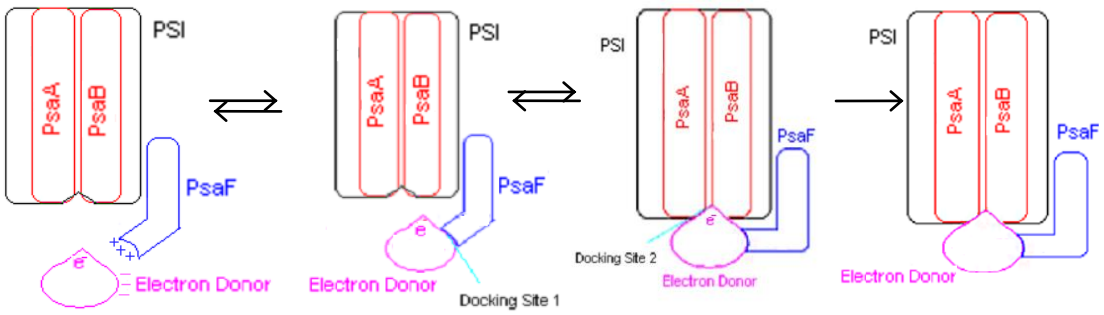

Figure 26: (A) Distant and close bound states of cyt c_{553} and P700.

the interface of cytochrome c_{553} and the photosystem complex core as the result of hydrophobic interactions between cyt c_{553} and PsaA and PsaB at ”Docking Site 2”.

The scheme given in Equation 12 includes two conformations of the Pc.P700 complex, with Pc bound in a 'close' (Pc.P700) or a 'distant' (Pc….P700) conformation, that are in equilibrium. It has been assumed that the close bound state is an obligate intermediate in the electron transfer from the distant bound state, i.e., the conformational change constitutes a rate-limiting step (determined by the rate constants k_{et} and k_c) [36, 43, 49]. The close and distant bound states should be thought of as two structures of a complex of Pc and P700 which lead to highly different rates of electron transfer and not in terms of well-defined distances. In the most general case, this model gives rise to three phases in the decay kinetics of $P700^{ox}$ but at high Pc concentrations one of these has a zero amplitude [43]. When going from a high to a low Pc concentration, the number of decay components is expected to increase from two to three. Therefore this model can be used at high Pc concentrations, where the possible inhibition by oxidized Pc can be neglected [43]. This scheme was obtained by putting forward the two following

alternative schemes made by Bottin and Mathis [61]. Fast reaction (close bound state, linear Model):

$$Pc(I)^r + P_{700}{}^o \longleftrightarrow Pc(I)^r .... P_{700}{}^o \longleftrightarrow Pc(I)^r . P_{700}{}^o \xrightarrow{12\mu s} Pc(II)^o . P_{700}{}^r , \qquad (18)$$

where Pc(I)= steady Pc
Pc(II)= exited Pc

Slow reaction (distant bound state, Parallel Model)

$$\begin{array}{ccc} \text{cyt } c_{553}(I)^r + P_{700} & \longleftrightarrow & \text{cyt } c_{553}(I)^r ....P_{700} \\ \downarrow & & \downarrow \\ \text{cyt } c_{553}(I)^r + P_{700}{}^e & \longleftrightarrow & \text{cyt } c_{553}(I)^r ....P_{700}{}^e \xrightarrow{110\,\mu s} \text{cyt } c_{553}(II)^o . P_{700}{}^r \end{array} \qquad (19)$$

Two different binding sites for Pc on P700 were assumed, a 'close' and a 'distant', with Pc reacting at each site according to model (16) but with different rate constants for the two sites. In particular, the decay lifetimes for ET was suggested to be 12 and 110 μ s for the distant and close bound states, respectively [61] .

It was assumed that two Pc molecules can be bound simultaneously to PSI and that the second, 'distant' bound Pc can donate an electron to P700 ^{ox}, either directly, or, via the 'close' bound one and the direct transfer alternative would then correspond to the parallel model.

Sigfridsson et al. [36] claimed that the parallel model could not account for their findings because it implies a monoexponential decay of $P700^{ox}$ at high Pc concentrations, with an apparent rate constant given by the sum of the ET rate constants for the two sites, contrary to their observed biexponential decay. However, it is possible that two Pc molecules can donate electrons to $P700^{ox}$ but then the ET from the 'distant' bound one has

to occur via the 'close' bound one in order to obtain agreement between the last two models [36].

Kinetic Analysis

It has been shown that the three rate constants for the first model (11) are related to the rate constants through [64]:

$$p = k_{on} + k_{off} + k_{et} \quad (20)$$

$$q = [p^2 - 4 (k_{on} k_{et})] \quad (21)$$

$$\tau_1 = (p + q) / 2 \quad (22)$$

$$\tau_2 = (p - q) / 2, \quad (23)$$

The sum and product of τ_1 and τ_2 yield the following additional relationships:

$$\tau_1^{-1} + \tau_2^{-1} = k_{on} [Pc] + k_{off} + k_{et} \quad (24)$$

$$(\tau_1 \tau_2)^{-1} = k_{et} k_{on} [Pc]. \quad (25)$$

The sum and product of τ_1^{-1} and τ_2^{-1} can be plotted versus [Pc] as follows:

$$y = ax + b \quad (26)$$

$$y_1 = a_1x_1 + b_1, \; y_2 = a_2x_2 + b_2 , \quad (27)$$

where

$$y_1 = \tau_1^{-1} + \tau_2^{-1}, \; a_1 = k_{on}, \; x_1 = [Pc] \text{ and } b_1 = k_{off} + k_{et} \quad (28)$$

$$y_2 = (\tau_1 \tau_2)^{-1}, \; a_2 = k_{et} k_{on}, \; x_2 = [Pc] \text{ and } b_2 = 0 \quad (29)$$

The slope of the sum of τ_1^{-1} and τ_2^{-1} versus [Pc] is k_{on}, and k_{et} can be calculated from the slope of the product of τ_1^{-1} and τ_2^{-1} versus [Pc]. The intercept of the sum represents the sum of k_{off} and k_{et} which is used to determine the value off k_{off} [64].

The three rate constants for the first model also can be found by using the above relationships (24) and (25) for the sum and product of τ_1 and τ_2 and the amplitude ratio, $A_1/(A_1 + A_2)$, as the third equation [35].

$$R = A_1/(A_1 + A_2) = [\tau_1^{-1} - k_{on}[Pc] - k_{off} - (k_{off}\, k_{et})/(k_{on}[Pc] + k_{off})]/(\tau_1^{-1} - \tau_2^{-1}) \quad (30)$$

In order to estimate the three rate constants; k_c, k_{et} and k_d, for the second model (12), three constants with respect to [Pc] are needed between all the amplitudes and lifetimes. In a first, exploratory step, the transients can be subjected to an analysis in which all the amplitudes and lifetimes are allowed to vary freely. The estimated τ_1 values are independent of the Pc concentration [36, 43]. The decay lifetime of the slowest component, τ_3, is also independent of the Pc concentration [36]. In a second step of the analysis, all absorption transients can again be subjected to a curve-fitting procedure, but now with τ_1 and τ_3 fixed at the average values. The relative contribution of the fast phase to the decaying kinetics, R, and τ_2 saturate at high Pc concentrations[36, 43, 49]. In order to describe the saturation quantitatively, τ_2 and R can be fit to hyperbolic functions $(\tau_{2max}[Pc]/(C_{\tau_2} + [Pc])$ and $(R_{max}[Pc]/(C_R + [Pc])$, where $\tau_{2\,max}$ and R_{max} denote the saturating values and C_{τ_2} and C_R are the Pc concentrations at with half the saturating levels are reached [36].

At high Pc concentrations, $\tau_1^{-1}, \tau_2^{-1}{}_{max}$ and the maximum amplitude ratio are related to the rate constants through the following equations [36, 43, 49].

$$\tau_1 = k_c + k_{et} \quad (31)$$

$$\tau_{2\,max} = k_d\, k_{et} / \tau_1 \quad (32)$$

$$[A_1/(A_1+A_2)]_{max} = \tau_{2\,max}/(k_c + k_d) \quad (33)$$

Kinetic Measurement Setup

The apparatus used by Hargrove consists of a frequency-doubled YAG laser to provide a short excitation pulse (5 ns) at 532 nm. Absorbance measurements were made using a xenon lamp as a light source in combination with a filter to remove all light except that in the absorbance peaks region. The probe light was focused on the cuvette and then refocused on the monochromator slit. A monochromator was mounted to a photomultiplier tube in combination with a high voltage supply mount. The voltage signal from the photomultiplier was monitored with an oscilloscope; timing was accomplished with a pulse generator that supplied triggering pulses to the laser and the oscilloscope. The time course from the oscilloscope was transferred to a personal computer [64].

An apparatus similar to what was described above was used by Hoganson et al.[35, 36, 43, 49, 63, 65] which was referred to by Sigfridsson et al. [35, 36, 43, 49, 63, 65]. The excitation pulse was from a frequency-doubled Nd:YAG laser at 532 nm with 10 ns pulse duration. A diode laser passed a measuring beam at 830 nm through the sample onto an Si photodiode. A filter protected the photodiode from fluorescence and scattered light. The output from the photodiode was amplified and fed into an oscilloscope. The oscilloscope trace was captured by a digitizing camera system connected to a personal computer used for data treatment and storage.

The chosen flash photolysis setup is schematically shown in Figure 27. PSI is photo-oxidizedis by short (5-10 ns) flashes (532 nm) from a 450 mJ/pulse Nd:YAG laser. A Xe arc lamp can provide the measuring light at 830 nm which needs to be followed by a monochromator to remove wavelengths that are not in the absorbance peaks region.

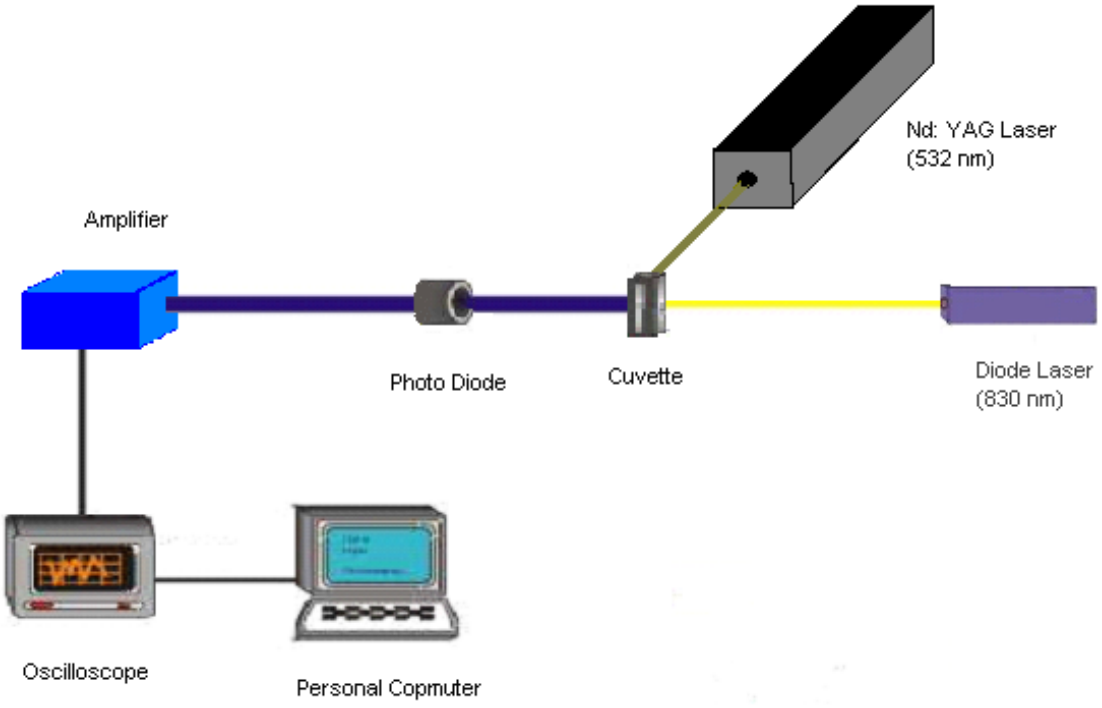

Figure 27: Flash photolysis apparatus

Therefore, a diode laser is more desirable for this purpose since it is cheaper and provides a stronger beam at a specific wavelength. The light passes through the cuvette holding the sample and impinges on a photodiode which produces an electrical signal. A photomultiplier tube can be also be used to produce signal, but it is more expensive than photodiode and since it is more sensitive at low light, it saturates at lower light level than a photodiode. Photodiodes are more sensitive to narrow band of light than photomultiplier tubes and are therefore more desirable for use in this system. The output from the photodiode is amplified and captured on an oscilloscope. The oscilloscope is connected to a personal computer to store data.

As it was discussed earlier, the flash-excitation of a mixture of PSI particles and cyt c_{553} results in an instantaneous absorption increase at 830 nm due to the photooxidation of P700 followed by a multiphasic decrease due to the reduction of P700 by cyt c_{553} (the fast phase reflects the oxidation of the reduced cyt c_{553} that is already bound to the reaction center complex and slower phase reflects complexes of reduced cyt c_{553} and P700 prior to electron transfer).

The flash artifacts, obtained by blocking the measuring light, are subtracted from the transient absorbance signals. Three exponentials are fitted to the signals by curve-fitting and three amplitudes and three half-lives will be obtained. The analysis will be made at high concentrations of cyt c_{553} in terms of the model (34).

$$\text{cyt } c_{553}^{\,r} + P_{700}^{\,o} \underset{k_{off}}{\overset{k_{on}}{\rightleftarrows}} \text{cyt } c_{553}^{\,r} \ldots P_{700}^{\,o} \underset{k_{c}}{\overset{k_{d}}{\rightleftarrows}} \text{cyt } c_{553}^{\,r} . P_{700}^{\,o} \xrightarrow{k_{et}} \text{cyt } c_{553}^{\,o} . P_{700}^{\,r} \qquad (34)$$

This model is preferred to be used because it describes the conformational changes of P700 and cyt c_{553} and the intracomplex electron transfer between them. And

three rate constants k_{et} ,k_c and k_d can be calculated by inserting the observed parameters, $\tau_1, \tau_{2\,max}$ and $[A_1/(A_1+A_2)]_{max}$, into the following equations.

$$p = k_{on} + k_{off} + k_{et} \tag{35}$$

$$q = [p^2 - 4\,(k_{on}\,k_{et})] \tag{36}$$

$$\tau_1 = (p + q) / 2 \tag{37}$$

$$\tau_2 = (p - q) / 2 \tag{38}$$

$$\tau_1 = k_c + k_{et} \tag{39}$$

$$\tau_{2\,max} = k_d\,k_{et} / \tau_1 \tag{40}$$

$$[A_1/(A_1+A_2)]_{max} = \tau_{2\,max}/(k_c + k_d) \tag{41}$$

However the following model described in Equation 42 can also be used for this approach if it results in biexponential decay of P700.

$$P_{700}^{\,o} \xleftrightarrow{200\,\mu s} \text{complex} \xrightarrow{20\,\mu s} P_{700}^{\,r}, \tag{42}$$

which 200 μ s and 20 μ s are the decay lifetimes for this reaction.

$$\text{cyt } c_{553}^{\,r} + P_{700}^{\,o} \underset{k_{off}}{\overset{k_{on}}{\rightleftharpoons}} \text{cyt } c_{553}^{\,r} \cdot P_{700}^{\,o} \xrightarrow{k_{et}} \text{cyt } c_{553}^{\,o} \cdot P_{700}^{\,r}. \tag{43}$$

An analytical solution for this scheme exists when the reaction starts with cyt c_{553} in large excess over P700. The extraction of the rate constants can be accomplished from τ_1 and τ_2 by using the following expressions for the sum and product of the two faster decay lifetimes.

$$p = k_{on} + k_{off} + k_{et} \tag{44}$$

$$q = [p^2 - 4\,(k_{on}\,k_{et})] \tag{45}$$

$$\tau_1 = (p + q) / 2 \tag{46}$$

$$\tau_2 = (p - q) / 2, \tag{47}$$

$$\tau_1^{-1} + \tau_2^{-1} = k_{on}[Pc] + k_{off} + k_{et} \tag{48}$$

$$(\tau_1 \ \tau_2)^{-1} = k_{et} k_{on}[Pc] \tag{49}$$

VITA

Mehrsa Raeiszadeh was born in Tehran, Iran on September 3, 1983. She graduated from Aboureyhan High School in Tehran, Iran in July of 1997. She attended Sharif University of Technology (Tehran, Iran) and received a Bachelor of Science from the Department of Chemical Engineering in December, 2005. She entered graduate school in August 2006 at the University of Tennessee, Knoxville. In August, 2006, she will receive a Master of Science from the Department of Chemical and Molecular Engineering.